Modelling Legacy Nitrogen Dynamics in the Transboundary Lake Erie Watershed

by

Meghan McLeod

A thesis
presented to the University of Waterloo
in fulfilment of the
thesis requirement for the degree of
Master of Science
in
Earth Sciences (Water)

Waterloo, Ontario, Canada, 2023

Author's Declaration

This thesis consists of material all of which I authored or co-authored: see Statement of Contributions included in the thesis. This is a true copy of the thesis, including any required final revisions, as accepted by my examiners.

I understand that my thesis may be made electronically available to the public.

Statement of Contributions

I would like to consider Dr. Nandita Basu and Dr. Kimberly Van Meter who contributed to the research summarised in this thesis. I would also like to acknowledge the contributions of Danyka Byrnes who tirelessly worked to provide me with the parameters and datasets for many model inputs used in this thesis and Shuyu Chang for her downscaling work.

Abstract

Lake Erie is a source of drinking water, recreation, and commercial opportunity for both the United States and Canada, making the protection of its water quality essential. In the past decades, Lake Erie's ecosystems have been adversely affected by recurring toxic algal blooms. These algal blooms are attributed to nitrogen (N) and phosphorus pollution from agricultural runoff. Despite recent efforts to reduce N application in the Lake Erie basin, high levels of N concentration persist in surface and groundwater systems. One of the reasons for this apparent stasis in N concentrations is legacy stores of N in landscapes that contribute to lag times in water quality response, even after inputs have ceased. Legacy N is stored in the soil and slow-moving groundwater and makes up a large portion of current N contamination. Quantifying these available legacy N stores is essential for creating nutrient reduction targets.

In this thesis, the variance of N inputs and legacy N across different sub-watersheds in the transboundary Lake Erie basin (LEB) are explored. First, I synthesised 2-century-long (1800-2016) N input and output datasets for 45 sub-watersheds across the basin. Specifically, I accounted for manure application, fertilizer, biological N fixation, domestic wastewater N, atmospheric N deposition, and agricultural N uptake. I then used the ELEMeNT modelling framework with these inputs to simulate N loading at the outlet for all 45 sub-watersheds and quantified N retention across the watershed over time. The models performed well overall with a median PBIAS of 1.9% (IQR: 0.7% -3.1%) and a median KGE (Kling Gupta Efficiency) of 0.75 (IQR: 0.66 to 0.88) between modelled and measured N loading across the sub-watersheds. Additionally, the models were able to simulate accumulated soil organic nitrogen (SON) values quite well, with a median PBIAS of 12.6% between modelled and measured SON.

The results show that N surplus (the difference between N inputs and non-hydrological N outputs) has been rising across most Lake Erie sub-watersheds since 1950 and has only started to plateau or decrease around 2000. Agricultural inputs from manure, fertilizer, and biological fixation were the lead contributors to N surplus in agricultural watersheds, and domestic N was the lead N contributor in urban sub-watersheds. Since 1950, between 4% and 44% of N has been stored as legacy N (23% median). On average 92% of this N legacy is retained in the soil and 8% is in the groundwater. Through correlation analysis I have found that higher fractions of groundwater N and SON legacy accumulation are correlated with slower travel times and lower tile drainage, while wastewater denitrification emerged as the dominant component in urban sub-watersheds. These results provide insight about drivers of legacy N and N release in sub-watersheds, which could aid in targeted nutrient management across the watershed.

Acknowledgements

I would like to thank Global Water Futures for providing me with funding throughout my degree. I am grateful for being able to work comfortably without financial worry for the past 2 years.

I would also like to thank my advisor, Dr. Nandita Basu, for allowing me to work with her and her incredible lab. Dr. Basu has taught me just as much about life as she has science. She encouraged me to stand up for myself and carve my own path. I will always be grateful for the confidence she has given me. I would also like to thank my mentors Danyka Byrnes, Lamisa Malik, and Dr. Kim Van Meter who have worked with and helped me throughout this project. Thank you for guiding me, brainstorming with me, and encouraging me. I have learned so much from you incredible women and am so lucky to have been welcomed into your nutrients team.

Thank you to Stephen and my family/friends for ensuring that I have had a work-life balance the past several years. I am so lucky to have had such an incredible support group to come home to. I love you all.

To the lab mates who I was lucky enough to become friends with, thank you for the late-night pep talks, memes, and laughs. You are the reason for my sanity. I hope to keep in touch, and I am always here for you if you need a listening ear.

Finally, I would like to thank the animals who provided me with emotional support throughout my many hours of working from home. Thank you, Nicki, Madi, Bella, Ms. Christie, and Phoebe. You are all good girls.

Dedication

This thesis is dedicated to Marie and Brian LeLievre.

Table of Contents

List of Figures

List of Tables

Chapter 1: Introduction

1.1 The nitrogen cycle in the Anthropocene

Today's global population is almost three times what it was a century ago (Roser, Ritchie, and Ortiz-Ospina 2013). Since the 1990s, human activity has dramatically altered the nitrogen (N) cycle, increasing global fluxes of reactive N by 70% (Galloway and Cowling 2021). As the human population grows and agricultural intensity increases, more manure and fertilizer are added to fields, usually in excess of crop nutrient requirements. These excess nutrients can pollute waterways. In the U.S., for example, it is reported that only half of the applied fertilizer is removed by crops, while the rest is left available to leach into water systems (Swaney, Howarth, and Hong 2018).

Excess N can have detrimental effects on surface and groundwater systems. N contamination in surface water contributes to eutrophication, creating hypoxic zones. Eutrophication is a global issue, affecting the ecosystems of fresh and saline water bodies (Wurtsbaugh, Paerl, and Dodds 2019) and their multitude of ecosystem services. Excess N can also severely contaminate groundwater. Drinking water provided by groundwater sources like wells and aquifers often exceeds the commonly recommended nitrate concentration of 10 milligrams per litre (EPA 2012). More than 20% of shallow wells sampled in the U.S. exceeded this limit (Dubrovsky et al. 2010). As global populations continue to increase, protecting the water quality of surface water and groundwater should be prioritized.

1.2 Human efforts to reduce nitrogen contamination

Several countries implemented efforts to mitigate the water quality effects of nitrogen pollution by setting targets to reduce point and non-point sources of nutrients. These nutrient reduction efforts ranged from the local to the international level (Le Moal et al. 2019; D'Elia et al. 2019; Iho et al. 2015). Europe introduced the Helsinki Commission, founded in 1970 to tackle algal bloom issues in the Baltic Sea. Their efforts inspired the Baltic Sea Action Plan (Helcom 2007), which outlines nutrient reduction plans for the watershed. Similarly, the United States launched the Gulf of Mexico Watershed Nutrient Task Force in 2008 to reduce the size of algal blooms in the Gulf by 2015 (Epa & OW 2014).

Despite global reduction efforts, N concentrations in coastal areas have remained steady or continue to increase, and groundwater N concentrations remain high in agricultural regions worldwide (Brookfield et al. 2021; Van Meter et al. 2015, 2016, 2017). One of the reasons behind this apparent stasis in N concentrations is legacy stores of N in landscapes that contribute to lag times in water quality response, even after inputs have ceased (Baily et al. 2011; Grimvall, et al. 2000; Van Meter et al. 2016).

1.3 Legacy nitrogen and time lags

Landscapes often accumulate nitrogen (N) from decades of N surplus. N surplus is equal to the difference between N inputs and non-hydrological N outputs. Inputs of N into the landscape include fertilizer, manure, wastewater, atmospheric deposition, and biological fixation, while non-hydrological outputs include crop removal and livestock grazing. While surplus N can exit the system through land denitrification or stream N export, a large fraction can remain in the system

and accumulate as soil organic N (SON) or mineralized groundwater N. This accumulated SON and groundwater N in the landscape is referred to as 'legacy' N (Van Meter et al. 2016; 2017).

Accumulation of legacy N can lead to time lags in water quality response after decreases in N application since the accumulated legacy can enter receiving water bodies long after inputs have ceased. Surplus N applied to the landscape interacts with groundwater and the soil profile, each of which can introduce long residence times between application and release. SON is most often the largest terrestrial pool of nitrogen (Jaffe 1992), while slow groundwater travel times contribute to the delayed release of N after it enters the groundwater. Figure 1 illustrates the potential pathways of surplus N in the landscape; some surplus has the potential to immediately and directly run off into surface water, but a considerable portion slowly travels through the soil and groundwater. Several studies have demonstrated legacy N and the associated time lags between N application and its hydrologic release. These time lags are not trivial; Meals et al. (2010) report some time lags ranging from the yearly to decadal scale. Vero et al. (2018) also reviewed N time lags across North America and Europe; suggesting that N turnover periods can reach up to a century in length due to legacy N and are highly influenced by the rise of commercial fertilizers. Further, Van Meter et al. (2016) investigated legacy N in the Mississippi River watershed. They modelled the accumulation of SON in the watershed over time and found that an estimated 53±25% of N inputs accumulate in the soil as SON.

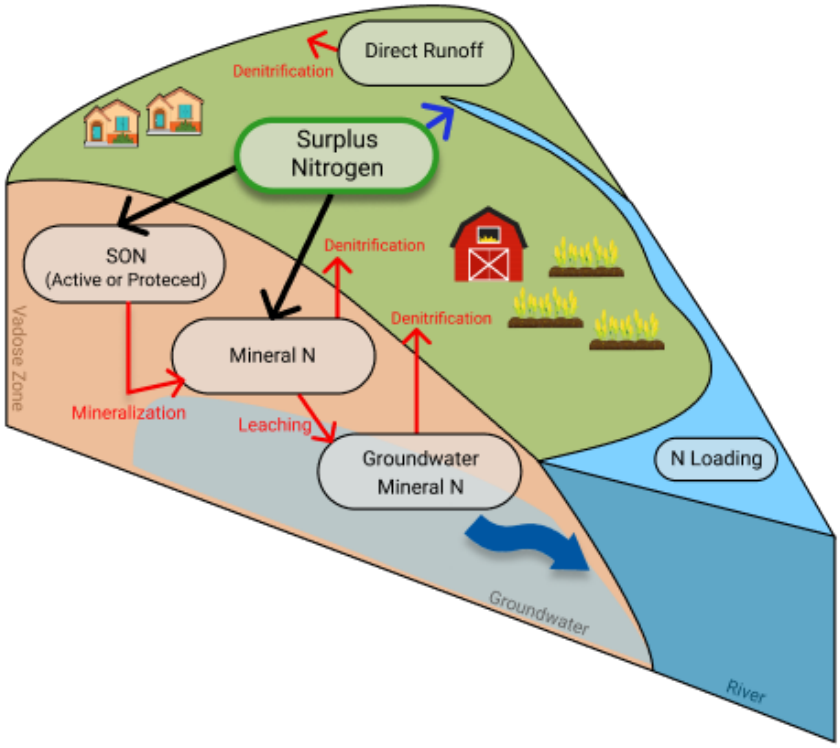

Figure 1: A conceptual diagram of nitrogen surplus pathways

While the existence of legacy N is well established in the literature, simulating this legacy computationally is relatively new. Many nutrient-polluted watersheds would benefit from models to quantify the amount of legacy N s.. This thesis aims to extend this field of work to quantify N legacies at the watershed scale.

1.4 Quantifying legacy N and current limitations

To plan realistic actions to reduce N pollution in watersheds, quantifying legacy N dynamics at the watershed scale is crucial. Stakeholders who make nutrient reduction strategies need to understand precisely how much of the N that contaminates water ecosystems was applied recently and what portion was applied decades ago. Measuring these N pools directly is not feasible; instead,

computational models are required to simulate accumulation dynamics to differentiate between legacy and recently applied N.

1.4.1 Building long-term N input/output datasets

To address N contamination concerns and to better understand long-term N dynamics, it is necessary to build long-term N input and output datasets that quantify exactly how much N is entering the landscape. Such long-term datasets are what allowed Van Meter et al. (2017) to run their models for the Mississippi and Susquehanna River basins in the United States described in section 1.4.3. On a larger spatial scale, Swaney et al. (2018) developed an N mass balance dataset covering the entire U.S., but at a much shorter time scale than covered by Van Meter et al. (2017). Most recently, Byrnes et al (2020, 2022) have created an N mass balance dataset for the contiguous U.S.. The dataset covered both a large spatial scale (the entire contiguous U.S., discretized to the county scale) as well as a long-time scale (1930-2017, discretized to the annual scale). There are also Canadian scale N mass balance studies, such as the residual soil nitrogen (RSN) indicator model developed by AAFC (Drury et al. 2007), which includes an agricultural N mass balance. Similarly, Karimi et al. (2020) calculated an updated national N mass balance for Canada. Even more recently, McCourt & MacDonald (2021) completed a provincial N footprint assessment in Canada to estimate drivers of reactive N emissions across Canada. In a recent study, Hamlin et al. (2020) developed the Spatially Explicit Nutrient Source Estimate Map (SENSEmap) which included N inputs to the landscape. However, this study only included the U.S. side of the transboundary Great Lakes and focused on a short timeframe of 8 years (2008 to 2015). In order to run models for watersheds that cross the Canadian and U.S. border, such as Lake Erie, data harmonization is required to capture long-term, spatially consistent N input/output trends.

1.4.2 Water quality modelling and legacy N

Several water quality models are available today which simulate nutrient fluxes at varying spatial and temporal scales. These water quality models can generally fall under two categories: empirical models and process-based models. Empirical water quality models rely on statistical relationships between nutrient inputs and outputs. These models establish regression relationships between the measured N applied to the landscape and its measured release into water bodies to simulate subsurface N fluxes. Examples of such models include SPARROW and Global NEWS (Chen et al. 2018). Process-based models use mechanistic equations to transform observed N applied to the landscape into N concentrations at the watershed outlet. Examples of these models include SWAT, HYPE, and HBV (Chen et al. 2018).

While several watershed models are theoretically capable of capturing N legacy dynamics, they are too computationally expensive and intricate to run at the century-scale needed to best capture long-lasting legacy stores and to model all subsurface pathways. Recently, some water quality models have been built specifically to capture legacy N pools and dynamics. Models that have been used to explicitly capture N legacies are the SWAT-LAG model, the LM3TAN model, and the Exploration of Long-tErM Nutrient Trajectories (ELEMeNT) model (Ilampooranan et al. 2019; Lee et al. 2014; Van Meter et al. 2017; Van Meter and Basu 2015). I aimed to choose a legacy modelling framework that can accurately capture legacy dynamics and has a simple enough framework to be applied across a large temporal and spatial space.

1.4.3 The ELEMeNT model

For this thesis, I used a model called ELEMeNT (Exploration of Long-tErM Nutrient Trajectories); a watershed nutrient legacy model which simulates N loading at the outlet as well as its legacy storage across the landscape. Details about ELEMeNT's modelling framework are provided in section 2.2.

The ELEMENT model has successfully been applied to several study sites in Europe and North America. The modelling framework was used to model N legacy dynamics in Germany's largest national river basin: the Weser River (Sarrazin et al. 2022). In the U.S., ELEMeNT was applied to the 2.9 million km^2 Mississippi River Basin (MRB) and the 70 thousand km^2 Susquehanna River Basin (SRB), two agriculturally dominated watersheds (Van Meter et al. 2017). With simulation periods of almost two centuries, both models utilized the watersheds' histories of N surplus to capture long-term legacy N stores. The models revealed that about 55% of the current N loading in the MRB and 18% of the current N loading in the SRB was older than 10 years old (Van Meter et al. 2017). This late release of legacy N has significant implications for the future health of the Gulf of Mexico (into which the MRB drains) and the Chesapeake Bay (into which the SRB drains). Even if N reductions are intense today in these areas, much of the N loading contributing to blooms will continue to be released from legacy sources.

More recently, ELEMeNT was applied to the Grand River Watershed (GRW) in Ontario, Canada (Liu 2020). The GRW is a 6800 km^2 agricultural watershed that drains into Lake Erie. The model, applied to several small watersheds across the watershed, revealed a spatial variation of legacy N

across the watershed, with 33% to 69% of surplus N is stored as legacy N and 49% to 72% of this legacy N is in the soil as SON across sub-watersheds.

1.5 Thesis objectives

The overall objective of this study is to understand nitrogen legacy dynamics across the transboundary Lake Erie basin. To achieve this objective, I (1) developed spatially-harmonized, long-term trajectory of N inputs and outputs for the Lake Erie basin, (2) built watershed models for several sub-watersheds across the basin to estimate N legacies, and (3) used model parameters to understand how landscape and management characteristics affect N legacy dynamics.

The process-based legacy N model ELEMeNT was applied to achieve this objective. This multi-watershed approach provides insight into how various soil, landscape, and climate patterns drive the legacy accumulation and depletion trajectories spatially across the basin.

2. Chapter 2: Methods and data sources

2.1 Study Area

Lake Erie is the shallowest, warmest, and has the most agriculturally dominated watershed of all the Great Lakes, with a volume of 484 cubic kilometres and a maximum depth of only 64 metres (Reutter, 2019). The lake's watershed stretches across the U.S./Canada border, is home to over 12 million people, and is severely human-altered (Us Epa 2014). With the increase in fertilizer use after WWII and intense agricultural activity, nutrient pollution in the Lake (including N) is a concern (Ho et al. 2017). Throughout the 1970s, Lake Erie experienced an extreme increase in nutrient concentration and still experiences recurring nutrient-induced eutrophication events today (International Joint Commission, 2014).

The Lake Erie basin (LEB) has undergone significant land use changes over the past century and its land cover varies spatially today. While the watershed includes several major cities including London ON, Kitchener ON, Detroit MI, and Cleveland OH; its main land use is agriculture, with the land modified immensely to meet growing agricultural needs (Figure 2). The watershed is also heavily tile-drained, with almost every region of the basin artificially drained to some extent. In addition to human modification, morphology and soil properties also vary across the basin.

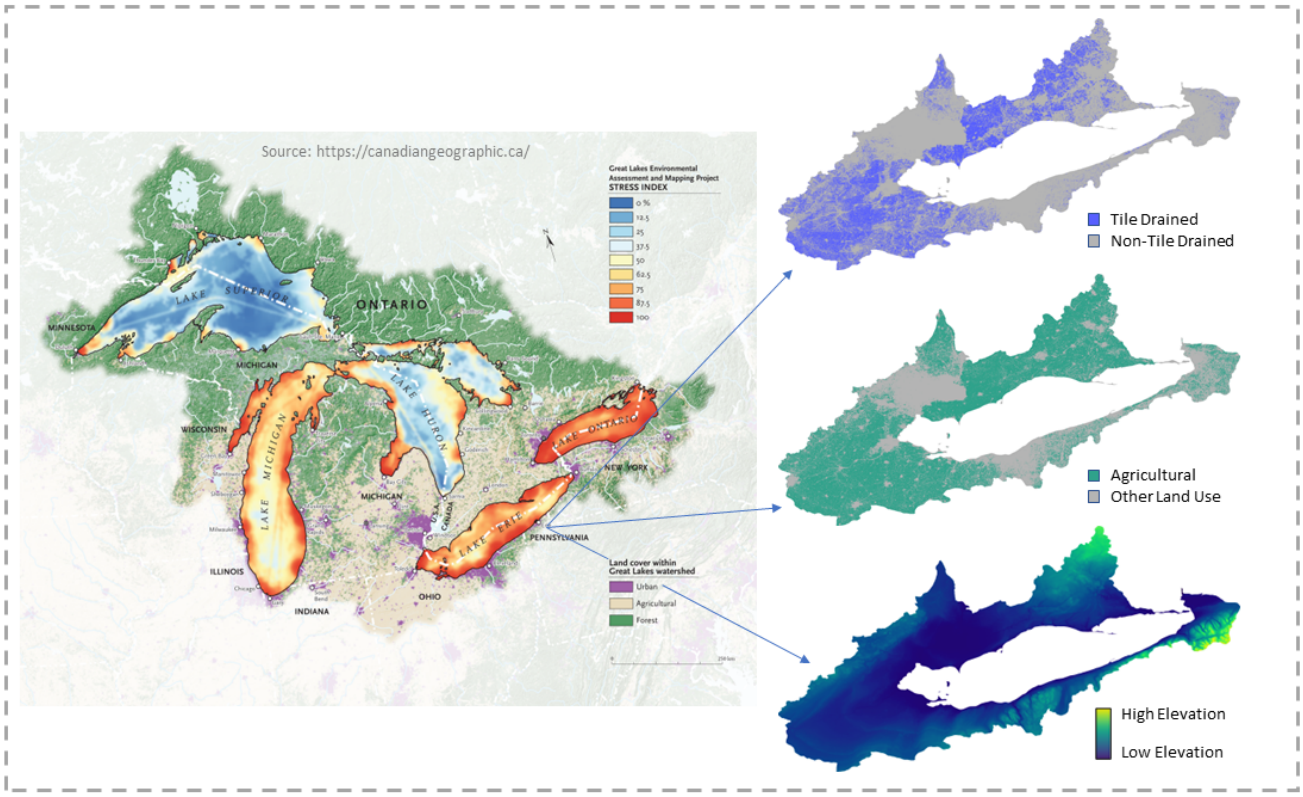

Figure 2: Spatial physical characteristics of the Lake Erie basin including land cover, tile drainage, agriculture, and elevation at 250m (Great Lakes Land Cover figure sourced from Canadian Geographic).

2.2 The ELEMeNT model framework

2.2.1 Overview of the ELEMeNT model

I will be utilizing the ELEMeNT model to simulate N storage and fluxes across Lake Erie's sub-watersheds. ELEMeNT (Exploration of Long-Term Nutrient Trajectories for Nitrogen) is a process-based, parsimonious model which simulates the source zone depletion dynamics in the soil and groundwater and of the transport of N using a convoluted groundwater travel time distribution (Van Meter et al. 2016). Uniquely, ELEMeNT does not break a watershed down into spatial units; rather, it breaks the watershed into non-spatial landscape units, where each unit experiences a distinct land use pattern over time. This breakdown allows ELEMeNT to maintain

the memory of land use types not for only its present time but for the entire simulation period while also remaining computationally efficient. This memory maintenance increases the accuracy of the simulation of legacy N over time.

A conceptual framework diagram of ELEMeNT is shown below in Figure 3. To model N loading at the watershed outlet, ELEMeNT treats the landscape like a bundle of stream tubes each with its own travel trajectory to the outlet. N loading [M/L^2/T] at the outlet of the watershed at time t [T], $M_{out}(t)$, is simulated using the following equation:

$$M_{out}(t) = \int_0^\infty J_s(t-\tau) f(\tau, t-\tau) e^{-\gamma\tau} d\tau + (1-\lambda_{pop}) W(t) \quad \textbf{(1)}$$

where $J_s(t-\tau)$ is the source zone function, describing the flux of N from the mineral soil pool to the groundwater [M/L^2/T], $f(\tau, t)$ represents the transient groundwater travel time distribution function with travel time τ [T], and γ is a constant describing hydrologic N removal through denitrification [T^{-1}]. Finally, W(t) is N from domestic waste [M/L^2/T] and λ_{pop} is a constant describing waste N removal through denitrification [-]. The details of these equations are further explained in sections 2.2.2 - 2.2.4.

As mentioned above, ELEMeNT breaks its modelled watershed into distinct land use units using a land use array, LU, which is built using the watershed's measured crop and pasture area fraction over time. Each unit, s represents an index in the land-use array, which spans over time t. Specifically, LU is built using the following equation:

$$LU(s,t) = \begin{cases} 1, & s \leq percent\ cropland \\ 2, & percent\ cropland < s \leq percent\ cropland\ and\ pastureland \\ 3, & s > percent\ cropland\ and\ percent\ pastureland \end{cases} \quad \textbf{(2)}$$

where s is each unit's index and t is time. Thus, the watershed, at each time step, has a distinct ratio of cropland, pastureland, or non-agricultural land.

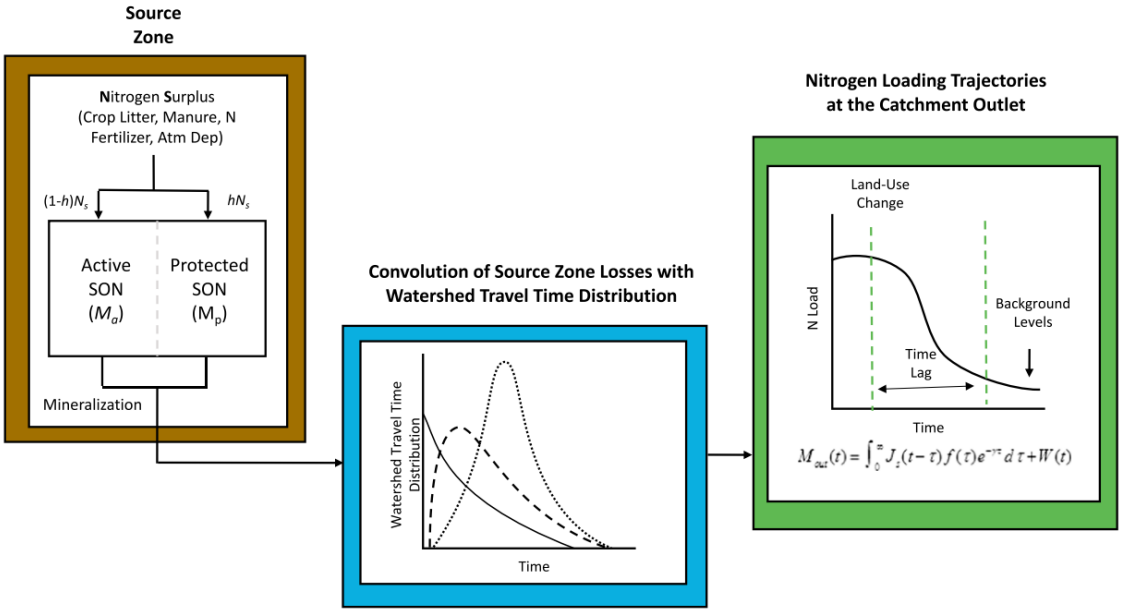

Figure 3: Conceptual ELEMeNT model framework for predicting catchment scale time lags as a function of hydrologic and biogeochemical legacies in the landscape**.** The source zone box illustrates the flow of N through soil organic matter. The middle box illustrates the convolution of mass from the source zone with the groundwater travel time distribution. Then, the right box describes N loading trajectories at the catchment outlet. (Source: Van Meter et al, 2017).

2.2.2 ELEMeNT model: source zone dynamics

2.2.2.1 SON in the source zone

Non-point sources of N surplus enter the source zone of the watershed. Here, N is stored as SON until mineralized into its inorganic forms and transported through the groundwater. SON in the source zone ($M_s(s,t)$) [M/L^2/T] can be broken down into its active and protected components: $M_a(s,t)$ and $M_p(s,t)$ respectively. Both pools undergo N accumulation and depletion, but the active pool has much faster kinetics than the protected pool which is more stable. The N dynamics for the active and protected SON pools vary across different land-use trajectory changes and are described by the following differential equations:

$$\frac{d}{dt}M_a(s,t) = \begin{cases}(1-h)N_s(s,t) - k_a M_a(s,t), & LU(s,t) \neq 1, LU(s,t-1) = 1 \\ (1-h)N_s(s,t) + \left(M_p(s,t) - 0.7M_{prist}\right), & LU(s,t) = 1, LU(s,t-1) \neq 1\end{cases} \quad \textbf{(3)}$$

$$\frac{d}{dt}M_p(s,t) = \begin{cases}hN_s(LU(s,t),t) - k_p M_p(s,t), & LU(s,t) \neq 1, LU(s,t-1) = 1 \\ hN_s(LU(s,t),t) + \left(M_p(s,t) - 0.7M_{prist}\right), & LU(s,t) = 1, LU(s,t-1) \neq 1\end{cases} \quad \textbf{(4)}$$

where $M_a(s,t)$ and $M_p(s,t)$ are the active and protected SON pools [M/L^2/T], $M_{p_{prist}}$ is the protected SON stocks under pristine land use conditions [M/L^2/T], and $N_s(LU(s,t),t)$ is the land-use-specific N surplus array [M/L^2/T] at time t [T] for LU type LU(s,t). Finally, h is a protection coefficient that mediates surplus N's partitioning into either the active or protected SON pools.

2.2.2.2 Mineralized N in the source zone

Eventually, N in the SON pool becomes mineralized ($M_s(s,t)$, [M/L^2/T]) and it can either undergo denitrification or leach into the groundwater. This process is summarized in the equation below:

$$\frac{d}{dt}M_s(s,t) = k_a M_a(s,t) + k_p M_p(s,t) - \lambda_s M_s(s,t) - J_s(s,t) \quad \textbf{(5)}$$

where $M_a(s,t)$ and $M_p(s,t)$ are the active and protected SON pools [M/L^2/T]; $k_a$and $k_p$are mineralization rate constants for the active and passive SON pools respectively [T^{-1}]; λ_s is a first-order soil denitrification rate constant [T^{-1}]; and $J_s(s,t)$ is the leaching flux to groundwater.

To calculate the flux of N from the mineral pool to groundwater ($J_s(s,t)$) [M/L^2/T], ELEMeNT models $M_s(s,t)$, the source zone mineral pool for each spatial unit at time t [M/L^2/T]

$$J_s(s,t) = \begin{cases} M_s(s,t)\frac{Q(t)}{V_w}, & Q(t) < V_w \\ M_s(s,t), & Q(t) > V_w \end{cases} \quad \textbf{(6)}$$

where $Q(t)$ is the annual stream discharge [L^3/T] and V_w is the volume of water in the soil column [L^3].

2.2.3 ELEMeNT model: travel time distribution

The groundwater flow of N, after it has leached from the source zone and flows as nitrate N, is modelled using a transient travel time distribution. I use a revised travel time distribution formulation, used by Sarizin et. al (2022). I assume complete mixing in the groundwater, and thus an exponential formulation for the travel time distribution:

$$f(\tau, t-\tau) = \frac{1}{\mu\prime(t)} e^{-\int_{t-\tau}^{t} \frac{1}{\mu\prime(x)} dx} \quad \textbf{(7)}$$

where $f(\tau, t-\tau)$ is the groundwater travel time distribution function, at time t [T] with travel time τ [T]. The mean of the travel time distribution, $\mu'(t)$ [T], is calculated using the following equation:

$$\mu'(t) = \frac{\underline{Q} \cdot \mu_{sub}}{Q(t)} \quad \textbf{(8)}$$

where $\underline{Q}$ is mean discharge at the outlet [L/T], $Q(t)$ represents discharge at the outlet at time t [L/T], and μ_{sub} is the harmonic mean [T] of $\mu'(t)$.

2.2.4 ELEMeNT Model: domestic wastewater input

The final component of ELEMeNT's main flux equation (1) is wastewater N (W(t)). Domestic waste N over time is obtained for each modelled sub-watershed using human population data and an estimated N excretion parameter of 5 kg/ha/year/person (described further in section 2.4.5). W(t) is multiplied by (1- λ_{pop}) where λ_{pop} is a constant describing the fraction of waste N removal through denitrification.

2.3 Model domain and water quality data

2.3.1 Sub-watershed gauge selection

In order to understand nitrogen legacy dynamics spatially across the LEB, I chose to study smaller sub-watersheds across the basin which had sufficient discharge and water quality data. Gauge data for water quality and discharge are provided by the Provincial Water Quality Monitoring Network (Ontario Ministry of Environment, Conservation, and Parks 2020) and the

Canadian Hydrometric Database (National Hydrological Service, 2016) respectively for the Canadian portion of the watershed, and by the USGS (US Geological Survey, 2020) for the watershed on the U.S side of the border. The U.S. dataset was supplemented with stream gauge data from the Michigan Department of Environmental Quality (MIDEQ) and the Ohio Environmental Protection Agency (OHEPA). The gauges on the U.S side of Lake Erie have N concentration data and flow data that are co-located. The Canadian side, however, separate gauges are maintained for flow and concentration data. Thus, for each Canadian sub-watershed, a water quality gauge and a flow gauge were paired. Paired gauges were chosen based on the following criteria: at most a 10% discrepancy between the drainage area for both gauges a minimum of 10 years of overlapping data for both gauges, and at least 25 years of flow data. Table 1 presents a finalized list of all of the sub-watersheds studied in this thesis. There are a total of 45 sub-watersheds: 25 in Canada (8 non-nested) and 20 in the US (14 non-nested). Each sub-watershed has been given a short form: 'Cx' for Canadian basins and 'Ux' for U.S sub-watersheds. These short forms are used throughout this thesis, and this table can be used as a reference. Additionally, the location of these sub-watersheds and their gauges are visualized in Figure 4.

Table 1: List of all studied sub-watersheds

Canadian Sub-watersheds		**U.S Sub-watersheds**	
Watershed Name	**Drainage Area [km^2]**	**Watershed Name**	**Drainage Area [km^2]**
North Thames River Below Fanshawe Dam (**C1**)	1416	Clinton River At Sterling Heights, MI (**U1**)	309
North Thames River Near Thorndale (**C2**)	1337	Clinton River At Gratiot Avenue,, MI (**U2**)	734

Thames River At Thamesville (**C3**)	4540	River Rouge At Detroit, MI (**U3**)	187
Thames River At Innerkip (**C4**)	150	Huron River At Ann Arbor, MI (**U4**)	729
Sydenham River Near Alvinston (**C5**)	704	River Raisin Near Monroe, MI (**U5**)	1042
Big Otter Creek Above Otterville (**C6**)	99	Auglaize River Near Fort Jennings, OH (**U6**)	332
Big Otter Creek At Calton (**C7**)	655	Auglaize River Near Defiance, OH (**U7**)	2318
Big Creek At Walsingham (**C8**)	565	Maumee River Near Defiance, OH (**U8**)	5545
Lynn River At Simcoe (**C9**)	140	Maumee River At Waterville, OH (**U9**)	6330
Nanticoke Creek At Nanticoke (**C10**)	179	Honey Creek At Melmore, OH (**U10**)	149
Grand River At Galt (**C11**)	3487	Rock Creek At Tiffin, OH (**U11**)	35
Grand River At Brantford (**C12**)	5100	Sandusky River Near Fremont, OH (**U12**)	1251
Nith River At New Hamburg (**C13**)	549	Huron River At Milan, OH (**U13**)	371
Speed River Below Guelph (**C14**)	526	Vermilion R Nr Vermilion, OH (**U14**)	262
Speed River (**C15**)	547	Black River At Elyria, OH (**U15**)	396
Grand River Below Shand Dam (**C16**)	788	Rocky River Near Berea, OH (**U16**)	267
Grand River Near Marsville (**C17**)	665	Cuyahoga River At Independence, OH (**U17**)	707
Conestogo River At Glen Allan (**C18**)	573	Chagrin River At Willoughby, OH (**U18**)	246
Grand River At York (**C19**)	6015	Grand River Near Painesville, OH (**U19**)	685
Fairchild Creek Near Brantford (**C20**)	360	Cattaraugus Creek At Gowanda, NY (**U20**)	436
Mckenzie Creek Near Caledonia (**C21**)	174		

Speed River Near Armstrong Mills (**C22**)	176	
Eramosa River Above Guelph (**C23**)	232	
Grand River At West Montrose (**C24**)	1157	
Whitemans Creek Near Mount Vernon (**C25**)	397	

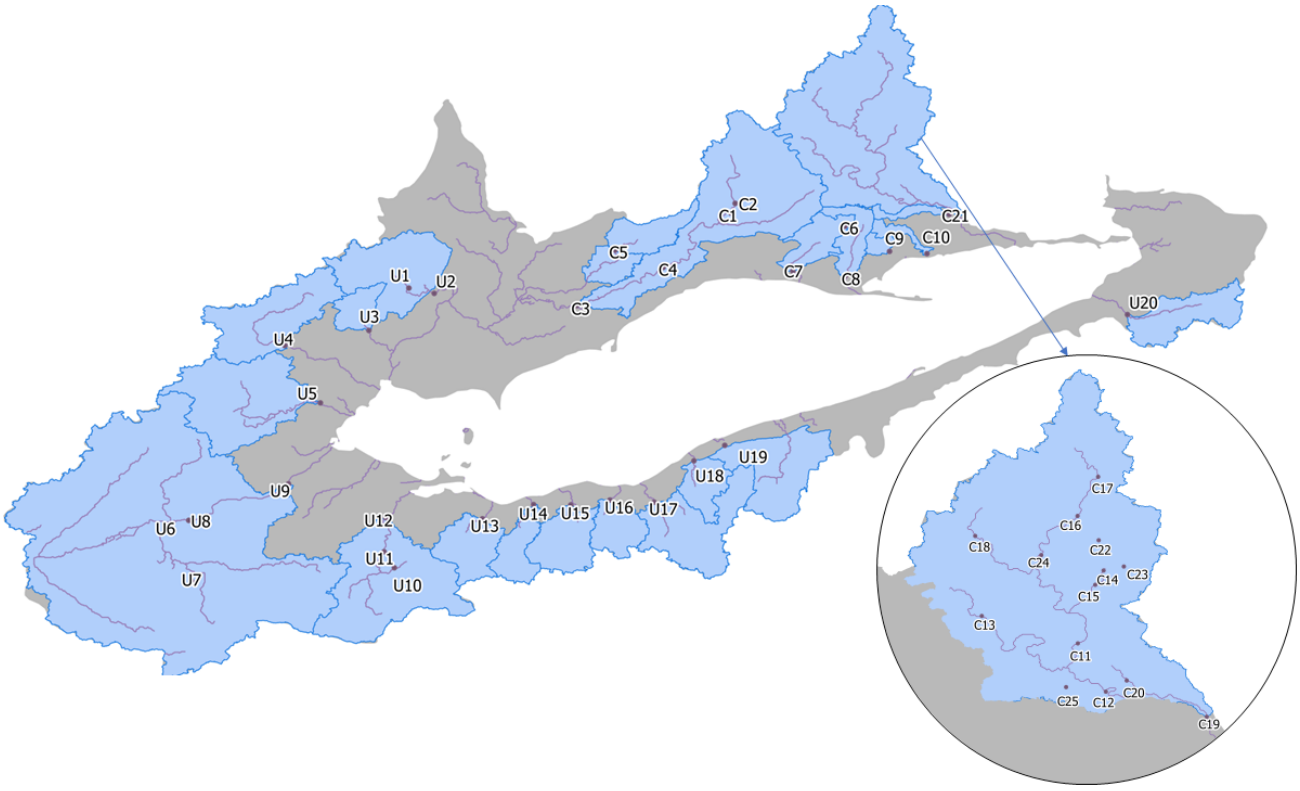

Figure 4: Lake Erie sub-watershed outlet locations including 20 gauging stations in the U.S. side of the Lake Erie basin, and 25 gauging station locations on the Canadian side, as well as associated non-nested sub-watersheds

2.3.2 Estimation of flow-weighted N concentration

For both the U.S. and Canada gauges, N concentration data is sparser than discharge data. Discharge is usually reported daily, whereas concentration data measurements are usually collected only a handful of times per year. To transform sparse concentration data to the daily scale, I used the WRTDS (weighted regression on time, discharge, and season) method (Hirsch, 2010). WRTDS estimates missing concentration data using available daily discharge data and is based on the following equation:

$$ln(c) = \beta_0 + \beta_1 t + \beta_2 ln(Q) + \beta_3 sin(2\pi t) + \beta_4 cos(2\pi t) + \epsilon \quad \textbf{(9)}$$

where the β's are regression coefficients, Q is streamflow, c is N concentration, and ε is an error term. By completing a WRTDS model for each sub-watershed, I obtained daily N concentration [M/L^3] and stream discharge [L^3/T], which are both used to calculate N loading [$M/L^2/T$].

2.4 Nitrogen inputs and outputs

To better understand long-term N dynamics, and to run the ELEMeNT model, it is necessary to build long-term N input and output datasets for the LEB. This section outlines each N input and output component, and how each was constructed. It should be noted that data comes from different sources across the Canadian-US border. Thus, harmonization was required. I used the TREND dataset for the US side of Lake Erie (Byrnes et. al, 2020; Byrnes et. al, 2022). The TREND dataset is a county-scale N input (fertilizer, manure, fixation, and deposition) and output (crop uptake) dataset from 1930 to 2017. For the Canadian side of the watershed, I developed methods to retrieve each N component in a way that was consistent with the TREND dataset. The data sources used, and their details are summarized in Appendix A**.** Annual N inputs include biological N fixation, livestock manure N, atmospheric N deposition, mineral N

fertilizer, and N from domestic waste. Annual non-hydrological N outputs consist of agricultural N crop uptake and livestock pasture N consumption. I refer to N 'surplus' (N_s; $M/L^2/T$) which is the difference between these inputs and outputs, defined by following equation:

$$N_s = FERT + MAN + DEP + BNF + WASTE - CROP \text{ - GRASS} \quad \textbf{(10)}$$

where MAN refers to N from manure applied to the land [$M/L^2/T$]; FERT refers to mineral fertilizer N applied to the land [$M/L^2/T$]; BNF refers to biological N fixation through vegetation [$M/L^2/T$]; DEP refers to atmospheric N deposition [$M/L^2/T$], WASTE refers to N from human wastewater [$M/L^2/T$], CROP refers N removed from agricultural activity [$M/L^2/T$], and GRASS refers to N removed by the grazing livestock [$M/L^2/T$].

2.4.1 Biological N fixation

Biological N fixation (BNF) is the process by which nonreactive atmospheric N is fixed by plants and transformed into reactive forms of N [$M/L^2/T$]. Major N-fixing crops in the LEB are beans, alfalfa, hay, and soybeans. For U.S counties, BNF data was collected directly at the county scale via the TREND dataset in kg/ha/year [$M/L^2/T$] (Byrnes et al, 2020; Byrnes et. al, 2022). For Canadian counties, BNF [$M/L^2/T$] is calculated using the following equation,

$$BNF = P_{crop} \times N_{crop} \quad \textbf{(11)}$$

where P_{crop} is crop production [$M/L^2/T$] and N_{crop} is an N mass fraction fixation for each crop type [M/M]. Production data were obtained using crop area and yield data from Statistics Canada (Statistics Canada, 2016a & 2016d). Fixation rates were based on values used in TREND (Table 2).

Table 2: Crop-specific biological N fixation rates
(From Byrnes et al. 2020; Byrnes et al. 2022)

Biological N Fixation Rates	
Crop Type	**Fixation Rate [kg N/kg/year]**
Soybeans	0.0657
Alfalfa Hay	0.0310
Non-alfalfa Hay	0.0154
Beans	0.0395

2.4.2 Livestock manure N

Manure N (MAN) inputs represent all waste excreted from livestock. For U.S. counties, MAN was collected at the county scale directly from the TREND dataset in kg/ha/year [$M/L^2/T$]. For Canadian counties, MAN inputs were estimated using the same approach and were estimated using the following equation,

$$MAN = POP \times N_{excr} \quad \textbf{(12)}$$

where POP is livestock population [headcount/L^2/T] and N_{excr} is the N content of the manure generated per animal [M/headcount]. Livestock headcount data (POP) were provided by the Canadian Census of Agriculture (Statistics Canada, 2016a). N content (N_{excr}) conversion parameters for different livestock types were estimated based on conversion values used in TREND (Table 3). To account for the fluctuation in the weight of different livestock over time, I scaled a 2008 livestock N excretion parameter forward and backward in time using weight scale factors for each livestock type (also done in TREND). For the model, I then divided the livestock

into either unconfined or confined fractions (Kellogg et al, 2000; Smil, 1999) and assumed unconfined livestock manure was applied right onto pastureland and that unconfined livestock graze on pastureland grasses during one-third of the year. Loss due to volatilization was assumed to be 36% of the total mass of the manure (Smil, 1999).

Table 3: Livestock-specific N excretion parameters
(From Byrnes et al. 2020; Byrnes et al. 2022)

Manure N Parameters	
Livestock Type	**N excretion rate in 2008 [kg N/kg/year]**
Beef Cows	69.54
Milk Cows	151.73
Other Cows	61.64
Hogs and Pigs	13.8
Sheep and Lambs	7.45
Chicken (not broilers)	0.58
Broilers	0.41
Turkeys	1.24
Horses and Ponies	44.7
Goats	7.45

2.4.3 Atmospheric N deposition

Atmospheric N deposition is the process where reduced forms of N (ammonia) and oxidized forms of N (nitrates) are deposited to land from the atmosphere. For both the Canadian and U.S. sides of the basin, N deposition was extracted using a gridded N deposition dataset spanning

from 1950 to 2013 (Wang et al. 2017). Deposition, before 1850, was scaled back using emissions data from the Carbon Dioxide Information Analysis Center (Boden et al. 2009), and deposition for the years 2014-2016 was linearly extrapolated.

2.4.4 Mineral N fertilizer

Fertilizer N (FERT) is N applied to crops through synthetic mineral fertilizers. For U.S. counties, FERT was collected at the county scale directly from the TREND dataset in kg/ha/year [$M/L^2/T$]. For the Canadian side of Lake Erie, FERT estimates were obtained at the county scale from 1945 to 2016. Estimates for county-scale fertilizer use were based on fertilizer sales data from Statistics Canada (Statistics Canada, 2016b) and county-scale crop areas from the Canadian Census of Agriculture (Statistics Canada, 2016a). I assumed that all fertilizer sold in Canada in a year was applied to the land that year and also assumed fertilizer N was applied on cropland only after , as non-significant amounts were applied prior to World War II. For years without sales data (1945-1951), linear extrapolation was used to fill in the gaps. Fertilizer amounts were then allocated to cropland or pastureland for each year based on the fraction of crop and pasture.

2.4.5 Domestic waste N

Domestic waste (WASTE) is N entering the landscape from human waste. For U.S sub-watersheds, WASTE inputs were collected directly at the county scale from the TREND dataset in kg/ha/year [$M/L^2/T$]. For Canada, WASTE inputs were estimated using human population census data (Statistics Canada, 2016c) [$headcount/L^2/T$] and converted to N using annual N excretion rates (5 kg-N/cap/yr) (Hong, Swaney, and Howarth 2011), this rate was also used for the TREND dataset.

2.4.6 Agricultural N uptake and livestock N uptake

Crop N uptake ($CROP_{uptake}$) is the N *removed* from the soil by harvested crops. For U.S counties, Crop N uptake was collected directly at the county scale from the TREND dataset in kg/ha/year [$M/L^2/T$]. For the Canadian side of the basin, $CROP_{uptake}$ [$M/L^2/T$] was calculated using the following equation,

$$CROP_{uptake} = P_{crop} \times NC_{crop} \quad \textbf{(13)}$$

where P_{crop} is crop production harvested [$M/L^2/T$] of a particular crop and NC_{crop} is a N content fraction parameter for that particular crop [M/M]. Crop area data and crop yield data (mass of crop per crop area) were obtained from Statistics Canada (2016a, 2016d). Crop area data were collected every 10 years from 1901-1951 and then every 5 years after that. The N-content conversion values were estimated based on conversion parameters used in TREND and literature estimates for crops not included in the TREND framework (Table 4).

Table 4: Crop N uptake parameters
(From Byrnes et al. 2020; Byrnes et al. 2022; Hong and Swaney. 2013 (**))

Crop N Parameters	
Crop Type	**N Content [kg N/kg/year]**
Alfalfa	0.0252
Barley	0.0188
Beans	0.0592
Buckwheat	0.0190

Canola	0.0354
Corn for fodder **	0.0130
Corn for grain	0.0130
Flaxseed	0.0346
All hay	0.0252
Hay (non-alfalfa)	0.0110
Mixed grains **	0.0220
Oats	0.0183
Other Crops	0.0270
Peas **	0.0650
Potatoes	0.0036
Rye	0.0191
Soybeans	0.0592
Sugar beets	0.0020
Sunflowers	0.0286
Tobacco	0.0319
Triticale	0.0269
Turnips **	0.0160
Wheat	0.0190

The last surplus component is N removed from the land through livestock grazing (GRASS). For U.S. counties, GRASS was collected at the county scale from the TREND dataset in kg/ha/year [$M/L^2/T$]. For Canadian counties, GRASS [$M/L^2/T$] was obtained for each livestock type using the following equation:

$$GRASS = POP \times N_{cons} \times \frac{1}{3} \quad \textbf{(14)}$$

where I assume livestock graze $\frac{1}{3}$ of the year. Here, POP is the number of a specific livestock type [headcount] and N_{cons} is the N consumption rate for that livestock type [M/headcount] (Table 5). Total pastureland N uptake is the sum of all livestock consumption. Consumption parameters were chosen to be consistent with the TREND dataset methodology (Table 5).

Table 5: Livestock-specific N consumption parameters
(From Byrnes et. al, 2020; Byrnes et al. 2022)

Livestock N Parameters	
Livestock Type	**N consumption rate in 2008 [kg N/kg/year]**
Beef Cows	79.33
Milk Cows	195.61
Other Cows	70.32
Hogs and Pigs	20.12
Sheep and Lambs	8.89
Chicken (not broilers)	0.89
Broilers	0.76
Turkeys	1.97
Horses and Ponies	50.06
Goats	8.89

2.4.7 Downscaling model inputs

The Lake Erie agricultural N inputs and N outputs were collected at the county scale (as described in section 2.4.2-2.4.6) because census data are reported at this scale. The ELEMeNT model runs at

the sub-watershed scale; however, several of the sub-watersheds in this study are smaller than a single county. Downscaling county data is done to account for spatial variation of agricultural land at smaller scales and within counties. For the U.S. side of the watershed, I utilized downscaling work done by Chang & Byrnes et al (in review) where the entire TREND county dataset (Byrnes et. al, 2022) was downscaled to a 250m-by-250m grid. For the Canadian side of the watershed, I matched the downscaled TREND methodology and used the gridded Annual Crop Inventory (ACI) (Agriculture and Agri-Food Canada, 2016a) to map our county surplus component into gridded agricultural and non-agricultural grids. For years before 2011, I assumed the same distribution of agricultural land as in 2011, as the ACI is temporally limited. I could then convert our county-scale N input and output data to gridded datasets, where N was re-distributed only to areas with agricultural land rather than assumed constant across each county. Ultimately, after downscaling, I developed downscaled, gridded maps for mineral N fertilizer, crop N uptake, manure N, and biological N fixation (deposition was already gridded in its original form). These downscaled grids could then be clipped to any sub-watershed across the entire LEB to provide a more spatially precise estimate of N input and output data at the sub-watershed scale.

2.5 Watershed land use trajectories

In addition to N surplus inputs (section 2.4) and water quality inputs (section 2.3), ELEMeNT requires a historical trajectory of land use (LU) for each of the modelled sub-watersheds. This LU trajectory is what allows the model to break up N surplus inputs into its crop, pasture, and non-agricultural components. For each sub-watershed in our study area, I constructed a 316-year (1700-2016) LU trajectory, which summarized the proportion of land covered by crop, pasture, or non-agricultural land. To do this, I used census-reported crop and pastureland for 1930-2016. I then supplemented this data with the Historical Croplands Dataset (Ramankutty and Foley 1999)

which is a gridded global dataset modelling crop and pastureland area fractions yearly from 1700 to 2007. The average LU history across all of the Lake Erie studied sub-watersheds, is shown in Figure 5.

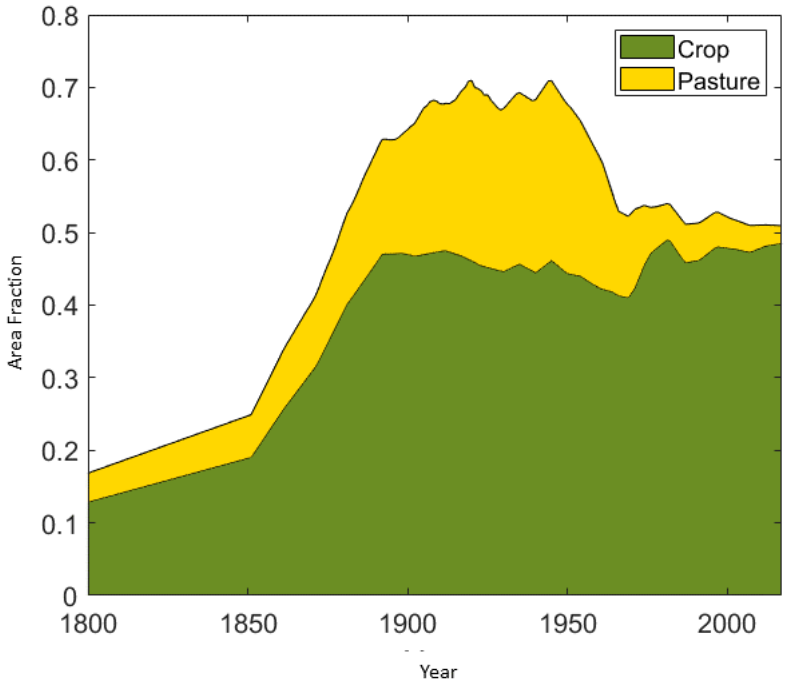

Figure 5: Land use trajectory for the Lake Erie basin including the average of cropland and pastureland area fraction trajectories for all 45 studied sub-watersheds.

2.6 Model parameter selection

2.6.1 Parameter range estimation

The ELEMeNT model requires eleven parameters that represent physical characteristics of the modelled watershed. These parameters and their details are summarized in Table 6. Of these parameters, eight are calibrated, two are based on measured soil data, and one is set constant based on literature values. I chose which parameters to calibrate based on a sensitivity analysis done by Liu et. al (2021).

Table 6: ELEMeNT model parameter descriptions

ELEMeNT Parameters		
Parameter	**Description [units]**	**Selection**
$\mathbf{M_s}$	Soil organic N content in pristine conditions [kg ha^{-1}]	**Calibrated**
$\mathbf{K_a}$	Mineralization rate of active soil pool [yr^{-1}]	**Calibrated**
$\boldsymbol{\lambda}$	Denitrification rate constant for soil [yr^{-1}]	**Calibrated**
$\mathbf{h_c}$	Cultivated humification rate constant [-]	**Calibrated**
$\mathbf{h_{nc}}$	Non-cultivated humification rate constant [-]	**Calibrated**
$\boldsymbol{\mu}$	Mean travel time [yr]	**Calibrated**
$\boldsymbol{\lambda_w}$	Denitrification rate constant for groundwater [yr^{-1}]	**Calibrated**
$\boldsymbol{\lambda_{pop}}$	Denitrification rate constant for wastewater [yr^{-1}]	**Calibrated**

s	Soil Saturation [-]	**Measured**
n	Porosity [-]	**Measured**
bnf_n	BNF net inputs in pristine conditions [kg/ha]	**Literature (Cleveland et al. 1999)**

Non-calibrated parameters were chosen using measured data available for each sub-watershed. Soil saturation (s) and porosity (n) were calculated for each sub-watershed using watershed-averaged soil attributes from the Soil Landscapes of Canada database (Agriculture and Agri-Food Canada, 2016b) for Canadian sub-watersheds and the USGS Soil Properties Dataset for U.S. sub-watersheds (Boiko et. al, 2021). Pristine biological fixation (bnf_n) was set constant to 3 kg/ha across all sub-watersheds (Cleveland et al. 1999).

Any calibrated parameters should be constrained by reasonable parameter ranges. These ranges are summarized in Table 7. I chose these ranges based on the Grand River Watershed (GRW) work done by Liu et al. (2021), where each range was selected using a data-driven and literature-based approach. The only parameters which had wider ranges than those used by Liu et al. (2021) were M_s (pristine SON content) and λ_{pop} (wastewater denitrification). M_s was given an upper limit of 19,000 kg/ha because several sub-watersheds in the LEB have a much higher SON stock than the GRW (Liu et al. 2021); specifically for the U.S. side of the watershed. Similarly, in consideration of the urban nature of some of the Lake Erie sub-watersheds outside of the GRW, the upper limit of λ_{pop} was raised to 0.95 to account for extensively urban sub-watersheds with more sophisticated wastewater treatment plants.

Table7: ELEMeNT model parameter calibration ranges

Calibrated ELEMeNT Parameter Ranges			
Parameter	**Units**	**Lower Limit**	**Upper Limit**
$\mathbf{M_s}$	[kg ha^{-1}]	7250	19000
$\mathbf{K_a}$	[yr^{-1}]	0.09	0.17
$\boldsymbol{\lambda}$	[yr^{-1}]	0.25	0.75
$\mathbf{h_c}$	[-]	0.14	0.26
$\mathbf{h_{nc}}$	[-]	0.28	0.75
$\boldsymbol{\mu}$	[yr]	3	34
$\boldsymbol{\lambda_w}$	[yr^{-1}]	0.07	0.13
$\boldsymbol{\lambda_{pop}}$	[-]	0.56	0.95

2.6.2. Model calibration

For calibration, I used an optimization software called OSTRICH (Asadzadeh and Tolson 2013; Tolson and Shoemaker 2007). OSTRICH is a model-independent optimization tool that can utilize several different parameter optimization algorithms to select a set of best-performing model parameters. I ran OSTRICH 5 times, each time with 200 iterations for each of the 45 subwatersheds. Thus, each model was calibrated using a total of 1000 model iterations.

I chose 3 objective functions (1) maximize the Kling-Gupta Efficiency (KGE) of modelled vs measured N loading at the outlet (Gupta et al., 2009), (2) minimize the percent bias (PBIAS) of modelled vs measured N loading at the outlet, and (3) minimize the PBIAS between the modelled and measured current SON. The equations for these objective functions are listed below. The equation for KGE is

$$KGE(obs, sim) = 1 - \sqrt{(CC-1)^2 + (\frac{\mu_{sim}}{\mu_{obs}} - 1)^2 + (\frac{\sigma_{sim}}{\sigma_{obs}} - 1)^2} \quad \textbf{(15)}$$

where *obs* is the observed data; *sim* is the modelled data; CC is the Pearson correlation coefficient between obs and sim; μ_{sim} and μ_{obs} are the means of *sim* and *obs*; σ_{sim} and σ_{obs} are the standard deviation of *sim* and *obs*. In this case, *sim* and *obs* are modelled and measured N loading at the outlet respectively. A KGE of 1 indicates a perfect match between observed and simulated loads, and a KGE of -$\sqrt{2}$ indicates that the model only performed as well as the mean of the observed loads (Knoben et al. 2019). The equation for PBIAS is:

$$PBIAS(obs, sim) = \frac{\Sigma(obs-sim)}{\Sigma(obs)} \quad \textbf{(16)}$$

where *obs* is the observed data, and *sim* is the modelled data. In this case, *sim* and *obs* are modelled and measured N loading at the outlet for the second objective function (2), and modelled and measured SON content for the third (3). PBIAS ranges between 0% and 100%.

Given these objective functions, I chose to run OSTRICH using its built-in Pareto-Archived Dynamically Dimensioned Search (PA-DDS) algorithm. PA-DDS is a multi-objective search

algorithm, which searches for and generates parameter sets within a user-defined range of acceptable parameters. With each iteration of the algorithm, it chooses a 'dominating' solution that performs the best across all objective functions. It then randomly perturbs this dominating solution (within the accepted parameter range) for each OSTRICH iteration and compares the solution to the archived solutions. This perturbation search algorithm continues until OSTRICH has compiled a set of non-dominated solutions (parameter sets), as well as dominated solutions.

2.6.2.1 Acceptance criteria for calibrated parameter sets

After running calibrations, I obtained 1000 dominated and non-dominated parameter sets for each sub-watershed. The parameters I accepted into the model ensembles were chosen by setting acceptance criteria. The acceptance criteria were (1) KGE of N loading was at least 50%, (2) PBIAS of N loading was at most 10%, and (3) PBIAS of SON was at most 25%. For sub-watersheds that could not satisfy all three of these conditions, I accepted the top 15% of parameter sets with respect to N loading KGE. By running models with these selected ranges of parameters, I introduced a range of outputs that capture the inherent uncertainty the parameters possess.

Chapter 3: Results and discussion

In this section, I will describe the results of calculating long-term N input and output trajectories across the LEB at the sub-watershed scale, and of applying the ELEMeNT model to these sub-watersheds to capture N legacy effects. First, section 3.1 examines the inputs and outputs of N across all 45 studied sub-watersheds over time, as well as each sub-watershed's stream N concentration. Section 3.2 explores the performance of the 45 models after calibration with respect to their ability to model N loading at the outlet and current SON levels. Section 3.3 explores the variation in calibrated parameter values across the basin and how these values relate to measurable physical land characteristics. Finally, in section 3.4, I analyze the modelled legacy pools of N across the sub-watersheds to capture the spatial variation of legacy retention.

3.1 Nitrogen surplus and load trajectories

3.1.1 N Inputs and non-hydrological outputs across the basin

I developed century-scale trajectories for agricultural N input (fertilizer N, manure N, biological N fixation) and output components (crop uptake) across the entire LEB from 1930-2016 at a 250-m grid scale (Figure 6). Agricultural nitrogen input and output patterns varied widely across the basin, with higher inputs concentrated in the western end of the basin, around the Maumee (U9) sub-watershed and in the northern parts of the basin in southern Ontario, around the Thames (C3) and Grand (C19) sub-watersheds (locations mapped in Figure 4). These areas have high agricultural activity and thus it is reasonable to see the majority of agricultural N application and uptake here.

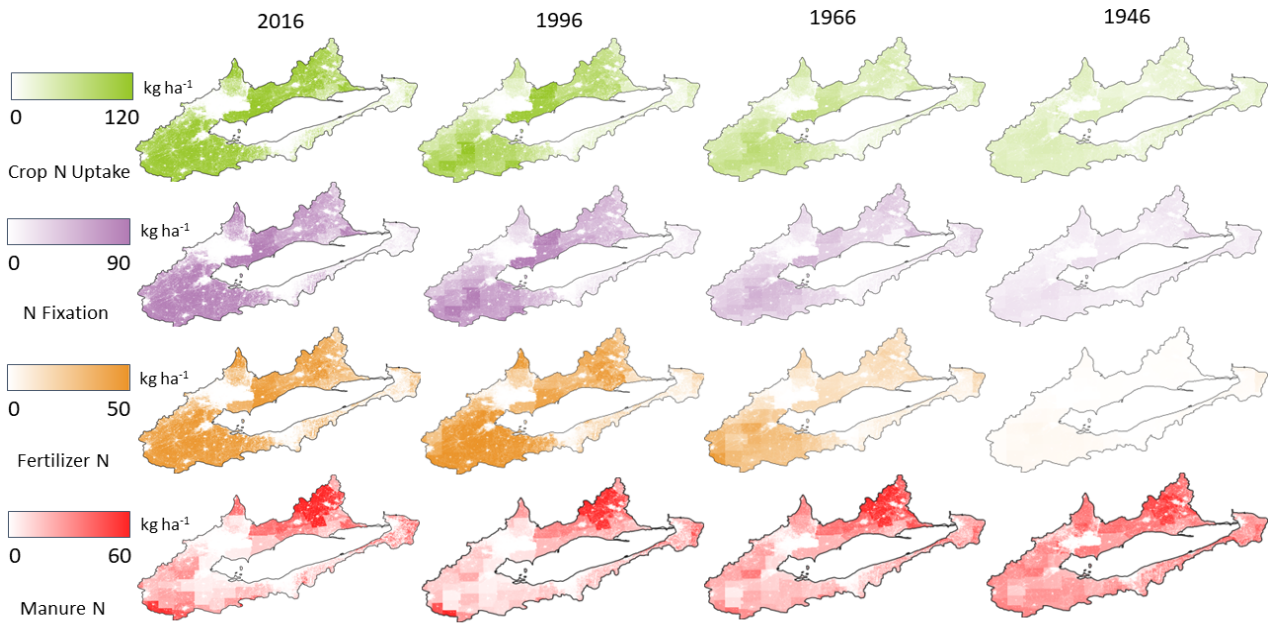

Figure 6: Downscaled agricultural N inputs and outputs in the Lake Erie basin over time. Four years of agricultural N surplus components across the LEB are shown (a subset of the annual 1930-2016 dataset) and these components include crop N uptake, N fixation, fertilizer N, and manure N. These data have been downscaled to a 250m^2 grid.

These agricultural input trajectories were used in conjunction with N deposition and domestic N use to estimate N surplus trajectories for each of the 45 sub-watersheds. Temporally, over the last 80 years, N surplus trends are similar: I see a relatively low N surplus (<20 kg/ha) across sub-watersheds until the period of 1950 to 2000, when N surplus increases noticeably. Then, I see a gradual decrease in N surplus across the sub-watersheds, where N continues to decrease or remain constant (see Figure 7g). While this general pattern is followed across the sub-watersheds, there is still a great deal of heterogeneity across the sub-watersheds. Peak N surplus levels vary from 34-108 kg/ha, and peaks occur in years between 1980-2001 among the 45 sub-watersheds. In 2016, surplus levels varied between the sub-watersheds. In 2016, N surplus across the sub-watersheds varies from 21 to 71 kg/ha.

The components of N surplus vary spatially and temporally across the LEB. Figure 7, shows the variation in N surplus components from 1930 to 2016 among the sub-watersheds. Fertilizer N application increased across all sub-watersheds after 1945, and gradually decreased or remained stagnant after 1980, but at different rates between the different sub-watersheds (Figure 7a). Fertilizer N application in 2016 varies from 0.04-73 kg/ha across the LEB sub-watersheds and got as high as almost 100 kg/ha. Crop uptake of N and biological N fixation trajectories also vary greatly across the sub-watersheds; crop N and BNF mostly increased across sub-watersheds throughout the modelling period; however, several sub-watersheds saw very little change in these categories or even experienced a decrease, likely due to urbanization (Figure 7b,f). Manure N application continuously increased for most sub-watersheds, but for some, manure N decreased after 1950 (Figure 7c). Manure N application in 2016 varies from 0.01-65 kg/ha. N from deposition followed the same pattern across the LEB sub-watersheds; it peaked in the 80s and then decreased significantly after that, likely due to a reduction in emissions (Figure 7d). Deposition in 2016 ranges from 7-12 kg/ha in 2016 but reached over 20 kg/ha at its peak in 1988. Crop uptake in 2016 ranges from 0.06-127 kg/ha in 2016. N from human waste is the smallest N surplus component for most sub-watersheds, however, for some of the urban watersheds, domestic N greatly increased over the modelling period; in 2016 domestic N waste ranges from 1.8-35 kg/ha. (Figure 7e).

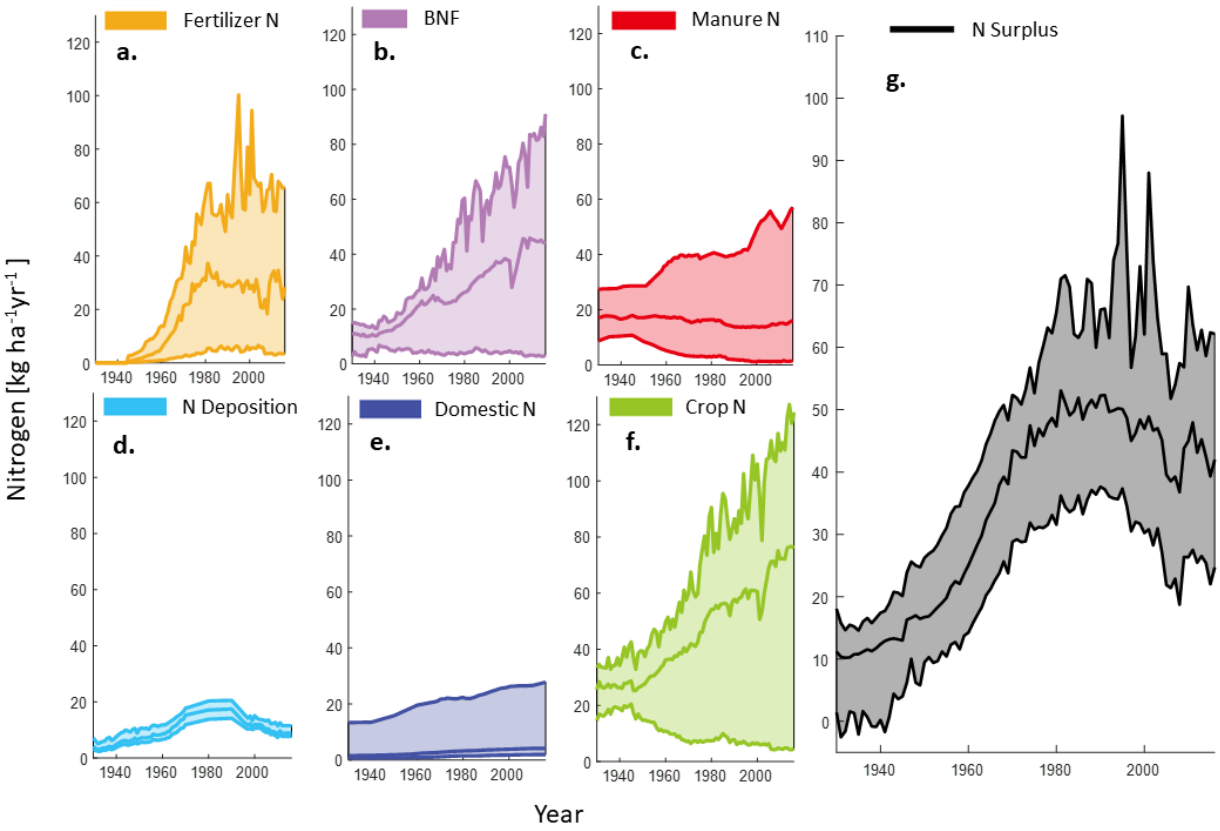

Figure 7: Percentile range [5%-95%] of N input and output trajectories for 45 studied Lake Erie sub-watersheds where N inputs include (a) fertilizer N, (b) biological N fixation, (c) Manure N, and (d) N Deposition. N outputs include (f) Crop N uptake. Surplus N (g) is the difference between N inputs and outputs.

To further demonstrate the variability of N surplus and their component trajectories, I highlight a sample of three sub-watersheds, one in Canada and two in the U.S. (Figure 8). The River Rouge sub-watershed (U3, close to Detroit, Figure 4) is mostly urban, and thus its surplus consists of very few agricultural inputs and outputs. Contrastingly, the Auglaize River sub-watershed (U7, Figure 4) in Ohio and Big Otter creek sub-watershed (C7, Figure 4) in Canada are predominantly agricultural, and so the surplus trajectories are mainly driven by fertilizer application, manure application, and crop uptake. Between the agricultural sub-watersheds, there is variation in surplus component magnitudes. The Auglaize River's surplus is dominated by fertilizer N inputs,

whereas Big Otter Creek's surplus is driven by manure, so, even while their surplus trajectory is similar in nature, the components of this surplus are drastically different. The decrease in surplus for the agricultural sub-watersheds is driven by an increase in crop uptake, while for the River Rouge, the decrease is driven by N deposition reduction (decreased emissions).

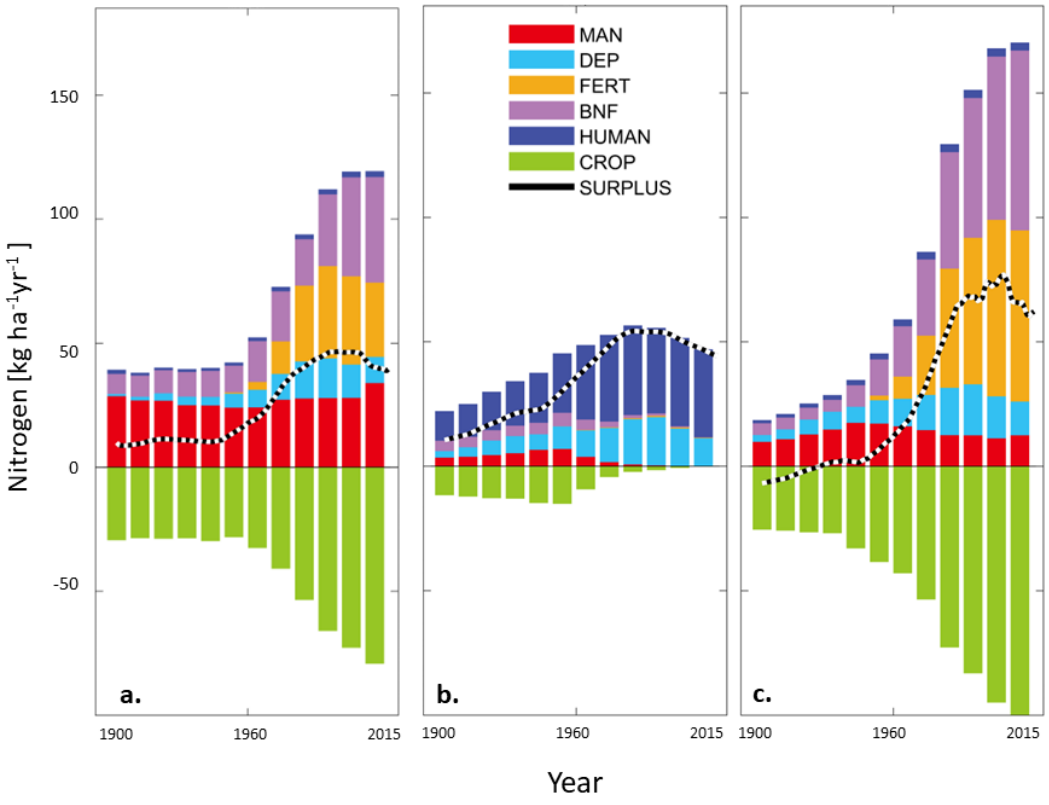

Figure 8: Watershed-scale N surplus trajectories and components for three Lake Erie sub-watersheds: (a) Big Otter Creek, (b) River Rouge, and (c) Auglaize River

3.1.2 Relationship between N surplus and hydrological N export

For each sub-watershed, I further examined how the annual N surplus o relates to annual hydrological N export (flow weighted N concentration at the stream outlet, FWC). Figure 9 shows that N inputs and hydrological N exports are decoupled across the LEB. In many of the

sub-watersheds I see a decreasing or stationary trend in N surplus, while N export continues to increase in this period (examples include the Lynn River (C9), Speed River (C15), and the River Raisin (U5), these locations are mapped in Figure 4). In other cases, I see just the opposite: a decrease in N export concentrations (FWC) but no corresponding reductions in N surplus (examples include the River Rouge (U3) and the Cuyahoga River (U17), these locations are mapped in Figure 4). These findings indicate the existence of 'legacy N' in the landscape (N stored for long periods of time in the soil and groundwater), which create a time lag between N application and N river concentrations. The variation in the application and release relationships across the various LEB sub-watersheds further demonstrates how the land cover and land use affect the release or retention of N in the system. To uncover the causes of this variability, I used a process-based modelling approach to simulate each sub-watershed's legacy and time lag dynamics and found spatially varying landscape controls on N retention and release.

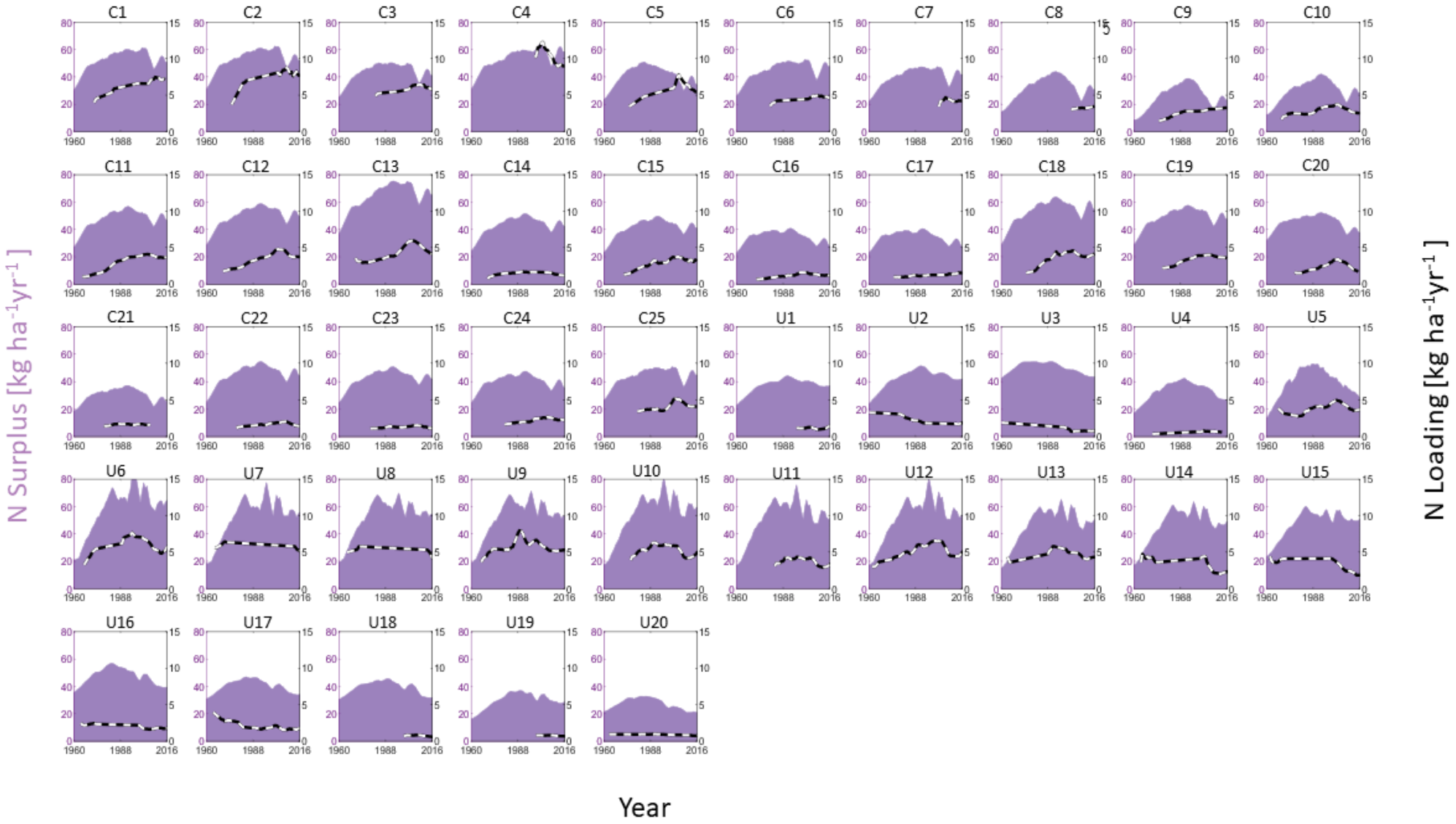

Figure 9: Surplus trajectories compared with flow weighted concentration (FWC) at the outlet for the 45 studied sub-watersheds in the Lake Erie basin between 1960 and 2016 (trajectories are plotted using a 3-year moving mean). Concentration is on the right y-axis (black), and surplus is on the left y-axis purple).

3.2 Model performance

We developed separate models for all 45 Lake Erie sub-watersheds using the ELEMeNT modelling framework. Inputs to the model included N surplus and its components (Section 3.1), model parameters, and land use data, while river load and concentration data were model outputs. Each sub-watershed was calibrated, and best-performing parameters were accepted and used to create a set of ensemble runs for each sub-watershed. The models were calibrated to the entire time period that N concentration data were available, to optimize the performance of the calibration.

3.2.1 Simulating N loading

The models were able to capture N loading patterns across all 45 sub-watersheds remarkably well, with a median KGE of 0.75 (IQR: 0.66 to 0.88), and a range of KGE from 0.18 - 0.91 (Figure 10), which is a very good performance for a parsimonious model (Ilampooranan et. al, 2019). The median PBIAS for loading was 1.9% (IQR: 0.7% - 3.1%), further confirming that despite some error in a few sub-watersheds, overall, the models were able to simulate N loading at the outlet very well. There were six sub-watersheds (U1, U3, U7, U14, U15, and U17) that had all of their ensemble KGE values less than 0.5. Sub-watersheds U1 (median KGE: 0.32) and U3 (median KGE: 0.44) are located near Detroit and are primarily urban, and this probably contributed to their low KGE values. Basins U7, U14, and U15 have large gaps in their observed loading data which might explain their low KGE scores (0.47, 0.18, and 0.42 respectively). Sub-watershed-specific load performance metrics are presented in Appendix B.

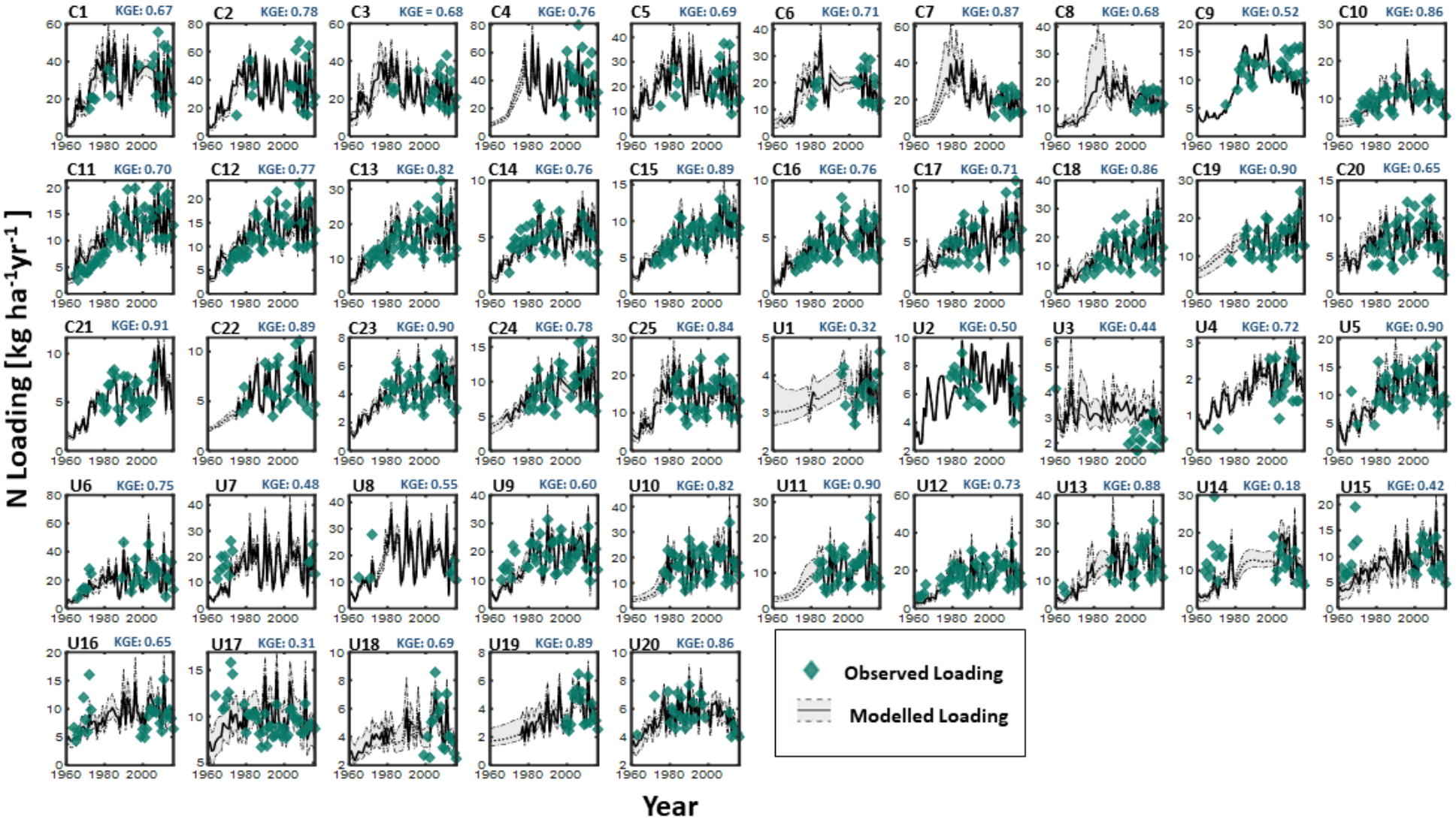

Figure 10: Modelled and measured loading at the outlet for 45 studied Lake Erie sub-watersheds from 1960 to 2016 [kg ha^{-1} y^{-1}]. The KGE values represent the median KGE value for each of the sub-watershed's ensemble runs. The black line represents the median loading for each sub-watershed's ensemble runs and the grey bounds are the ensembles upper and lower limit for loading. The green points represent measured N loading.

3.2.1 Simulating SON magnitudes

Each sub-watershed model was also calibrated to current-day SON values (Liu, 2013) using PBIAS as a metric. Generally, the models were able to simulate accumulated SON values quite well, with a median PBIAS of 12.6%. Figure 11 shows a plot of observed SON in 2011 against the median, modelled SON in 2011. Generally, the model was able to capture the higher SON accumulation for sub-watersheds with high measured SON values and captured lower SON accumulation in sub-watersheds with lower measured SON values.

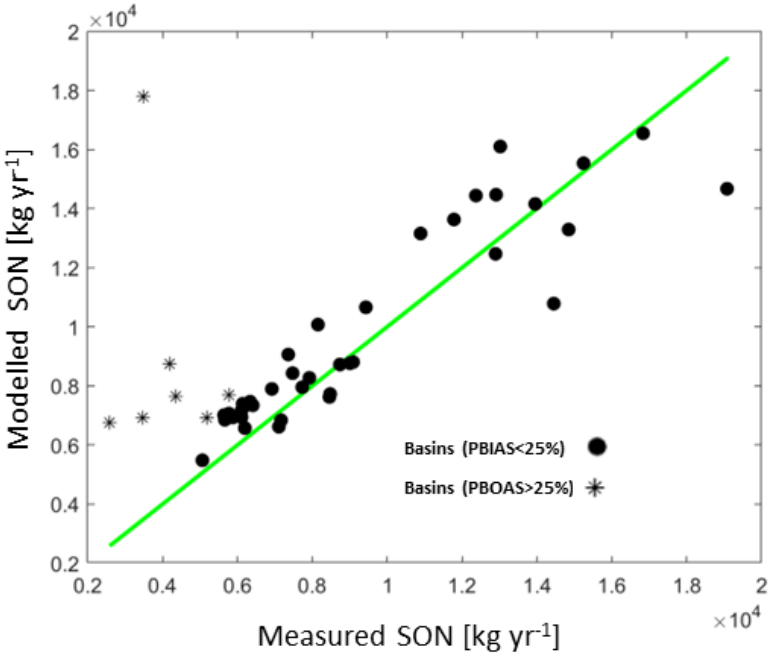

Figure 11: Modelled and measured SON for Lake Erie sub-watersheds in 2011. The solid circles represent sub-watersheds that had PBIAS between measured and modelled loading that was below 25% and stars are for sub-watersheds with PBIAS > 25%. The green line represents a one-to-one relationship between modelled and observed SON values

While most sub-watersheds fall close to the one-to-one line (where observed SON equals measured SON), there is still some deviation. Out of the 45 modelled sub-watersheds, there were 7 which did not meet the 25% PBIAS criteria are starred. This deviation between modelled and

measured SON exists for sub-watersheds with relatively low observed SON, for these sub-watersheds, the model overpredicted SON values. This error may be model related, but it is also possible that this mis-match is a product of limited SON data. While it would be ideal to have modelled and measured SON match perfectly, I expect some deviation as there exists uncertainty not only in the model but in the soil datasets from which observed SON was retrieved. The unified SON database, while harmonized across the U.S. and Canadian border, is quite coarse (0.25 degrees) and so, especially for smaller sub-watersheds, measured SON might be mis-represented. Sub-watershed-specific SON PBIAS metrics are included in Appendix B.

3.3 Relationship between watershed characteristics and key model parameters

While, in general, temporal trends in surplus were similar amongst the LEB sub-watersheds (section 3.1), I saw a much larger disconnect in temporal trends for modelled N loading and SON retention (section 3.2) which indicates that landscape heterogeneity likely plays a large role in how N inputs are retained and released. The parameter sets that each sub-watershed acquired through calibration also varied significantly across the LEB. This section aims to find relationships between these parameters and landscape characteristics in order to better understand how different landscape features drive modelled N fluxes.

Four parameters in the model are related to soil, groundwater and wastewater treatment plant (WWTP) denitrification: groundwater travel time μ, soil denitrification λ, groundwater denitrification λ_w, and wastewater denitrification λ_{pop}; these vary widely across the LEB (Figure 12).

Travel times range from 5 to over 30 years across the basin, indicating that some sub-watersheds store N in the groundwater for a longer period than others. Median soil denitrification rates range from 0.25 to 0.65 yr^{-1} across the sub-watersheds, and are greater than the median ranges for groundwater denitrification rate constants (0.07 to 0.12 yr^{-1}) . This is reasonable since denitrification in groundwater is often carbon limited, and thus lower. The proportion of human waste treated in WWTP ranges from 0.6 to 0.9, with higher values apparent for the more urban sub-watersheds, such as sub-watersheds U1-U4 near Detroit (Figure 4). This is reasonable given urban watersheds often have more advanced wastewater treatment plants, and lower proportions of septic wastes. Understanding what landscape features drive these parameter differences provides insight into how and why some sub-watersheds experience a higher N application to release lag time than others.

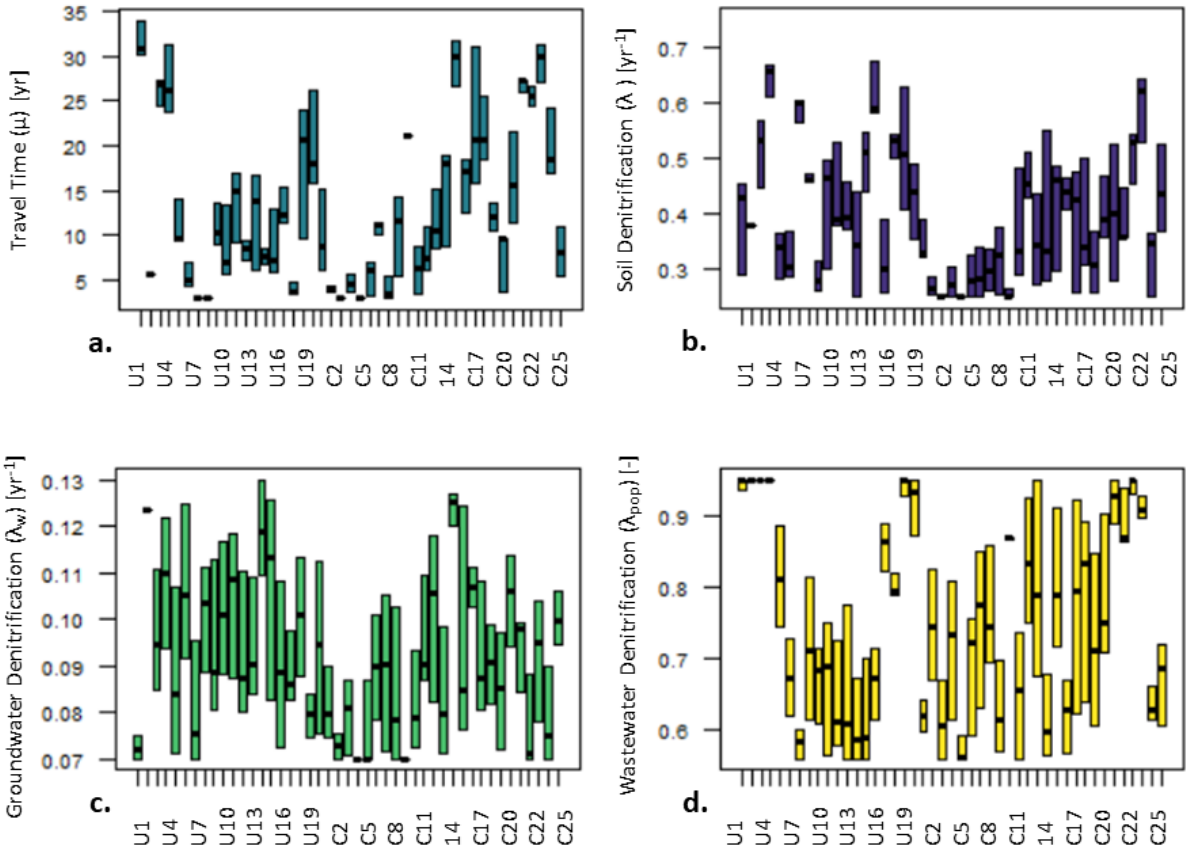

Figure 12: Calibrated rate parameter ranges across 45 sub-watersheds in Lake Erie. Each bar represents each calibrated sub-watershed's inter-quartile range for parameters: (a) travel time, (b) soil denitrification, (c) groundwater denitrification, and (d) wastewater denitrification

I found a significant negative relationship ($R^2 = 0.39$, $p < 0.0001$) between the mean travel time and fraction tiled area in a watershed, with greater travel times corresponding to areas with a higher tile drain area fraction (Figure 13a and Table 8). Tile drains are human-made artificial drainage systems put in place to remove excess surface water. As the density of watershed tile drains increases, N can flow quicker through the subsurface, most likely contributing to the negative relationship. This relationship with tile drains is similar to Liu et al. (2021), where in sub-watersheds across the Grand River (GRW), tile drainage percent was significantly negatively

correlated with mean travel time ($R^2 = 0.72$, $p = 0.02$). Liu et al. (2021) used only 14 sub-watersheds in their study, so it is interesting to see the same pattern persist across 45 sub-watersheds in Canada and the U.S. Like the GRW study, I also found a negative relationship ($R^2 = 0.16$, $p < 0.01$) between mean travel time and % silt and clay in the sub-watersheds (Table 8). This counter-intuitive relationship most likely arises because less permeable soils are preferentially drained by tile drains that contribute to shorter travel times. This suggests that human management systems, such as tile drains, have a greater affect on N fluxes than natural features like soil-type.

I also found significant negative relationships ($R^2 = 0.17$, $p < 0.01$) between the landscape scale denitrification rate constant (groundwater and soil denitrification) and the tile-drained area fraction (Figure 13b and Table 8). Higher tiled fractions lead to possible lowering of the water table that contributes to oxygenated soils and thus lower denitrification rates. Damkohler (groundwater denitrification rate multiplied by groundwater travel time) numbers showed a significant negative correlation ($R^2 = 0.38$, $p < 0.01$) with percent tiled areas, highlighting that tiled regions contribute to less N lost by denitrification due to both a hydrological effect (decrease of travel times) and biogeochemical effect (decrease of denitrification rate constant).

Finally, I see a significant positive correlation ($R^2 = 0.25$, $p < 0.001$) between population density and wastewater denitrification fraction (Figure 13c and Table 8). This is reasonable as in more urban watersheds with higher population densities, there tend to be larger, more sophisticated wastewater treatment plants, and thus a greater proportion of N is removed.

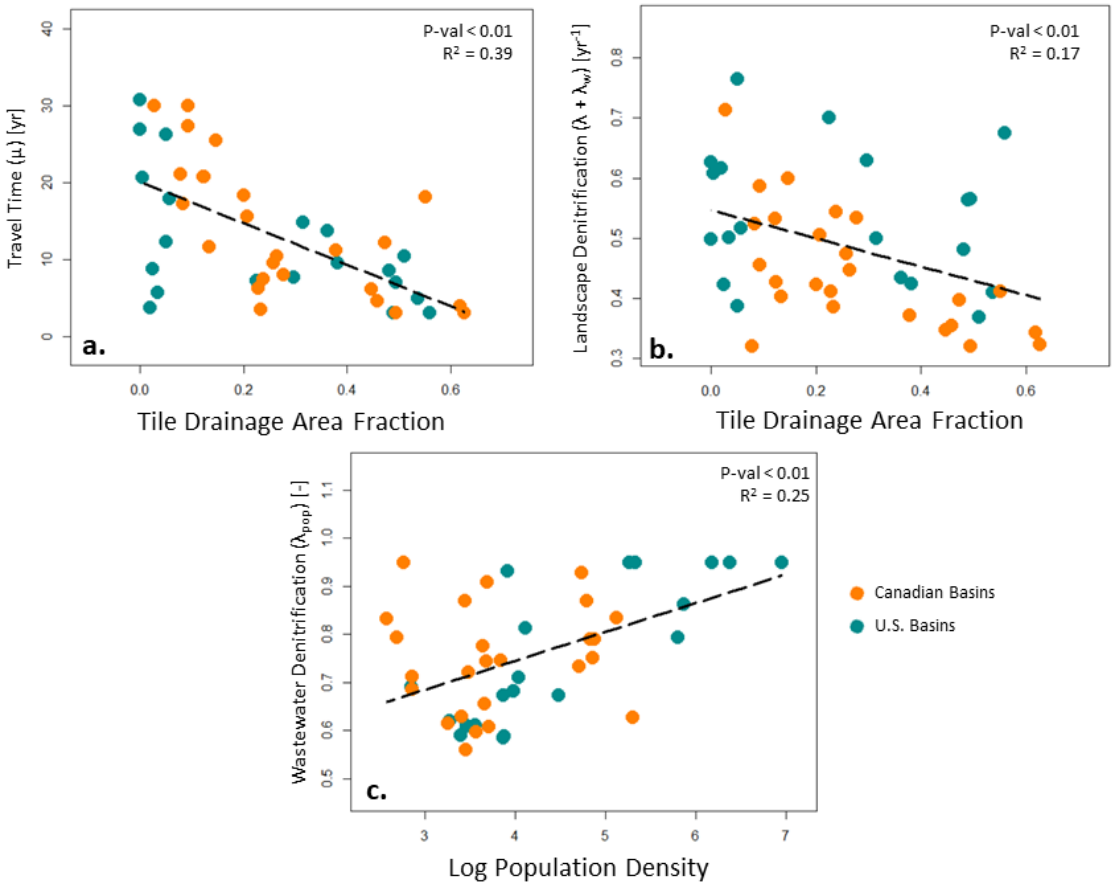

Figure 13: Correlation analysis between model parameters and watershed characteristics showing the relationships between (a) tile drainage and travel time (μ), (b) tile drainage and landscape denitrification (the sum of groundwater and soil denitrification, $\lambda_w + \lambda$) , and (c) log of population density and wastewater denitrification (λ_{pop})

Table 8: Correlation analysis summary for various landscape characteristics vs model parameters

A * indicates a negative relationship and **bold** indicates a significant relationship (p value < 0.05)

	R^2 (p value)					
Landscape Characteristics	GW travel time (μ)	Soil denitrification (λ)	Groundwater denitrification (λ_w)	Waste denitrification (λ_{pop})	Damkholer ($\mu \times \lambda_w$)	Landscape denitrification ($\lambda_w+\lambda$)
Tile Drained Area (%)	*0.39 (**<0.01**)	*0.16 (**<0.01**)	*0.05 (0.14)	*0.4 (**<0.01**)	*0.38 (<**0.01**)	*0.17 (<**0.01**)
Population Density Log	0.03 (0.27)	0.06 (0.11)	0.03 (0.28)	0.25 (<**0.01**)	0.03 (0.22)	0.06 (0.1)
Silt and Clay (%)	0.16 (**<0.01**)	*0.006 (0.62)	0.02 (0.38)	*0.17 (**<0.01**)	*0.10 (**0.02**)	*0.003 (0.7)

3.4 Modelled N fluxes and stores across the Lake Erie Basin

I next used the model results to quantify how N inputs on the landscape can be released into the river through N loading, stored as a legacy in the soil or groundwater, removed from the system via denitrification (soil or groundwater), or can undergo wastewater denitrification at WWTPs. The models were able to quantify how much N inputs have been stored as legacy N in the LEB. Notably, across the LEB, from 1950 to 2016, up to 910 kg per ha of N has been stored in the soil (median: 542 kg/ha) and as much as 187 kg/ha has been stored in the groundwater (median: 43 kg/ha). Together, this means that up to 952 kg/ha of N is stored as legacy in the studied sub-watersheds (median: 603 kg/ha). The relative proportions of these components varied across the LEB (Figure 14).

Over the last 66 years (1950-2016), across the sub-watersheds, 5-53% (median: 20%) of the cumulative N surplus was exported through the river network, 15% - 62% was removed via soil and groundwater denitrification (median: 44%), while 2% - 65% was released via wastewater denitrification (median: 6%). This leaves 4% - 44% of N stored as legacy N (median: 23%). On average 92% of this legacy N was in the soil and 8% was in the groundwater. These ranges are similar to an earlier study in the Grand River watershed (Liu et al. 2021) that found between 1930 and 2016, approximately 27% of cumulative N surplus had been exported to the stream, 35% was removed via land denitrification, 10% was lost through wastewater denitrification, and the remaining 30% was stored as legacy N.

Figure 14 shows the proportion of N stored and released during the 66-year period from 1950 to 2016 across the LEB as well as the cumulative N fluxes and stores for 3 major LEB sub-watersheds. While the breakdown of N surplus is similar to the GRW, the ranges for each component are widened across the entire LEB. This is likely due to the added variety in sub-watershed types added to this study. This analysis includes sub-watersheds that have a higher urban area fraction, lower agricultural urban fraction and a higher forest coverage than are present in the GRW. Thus, I are able to capture a wider range of accumulated N storage. Sub-watersheds U1-U3, for example, are three urban sub-watersheds near Detroit, so the majority of N applied to these watersheds is removed through wastewater denitrification, and their legacy N accumulation is very low. Since 1950, these urban sub-watersheds only have had 5% to 14% of their inputs stored as legacy N, while a cumulative 55% to 65% of N inputs were released via wastewater denitrification (much higher than in the GRW, where only about 10% of N was lost to wastewater denitrification). More agricultural sub-watersheds, like the Auglaize sub-watershed (U6), experienced a higher proportion of N storage like the GRW sub-watersheds. In the Auglaize River, for example, since 1950, 25% of N inputs remain in the system as legacy N. Across the entire LEB, as much as 43% and as little as <5% of N inputs have been stored as legacy N across different sub-watersheds.

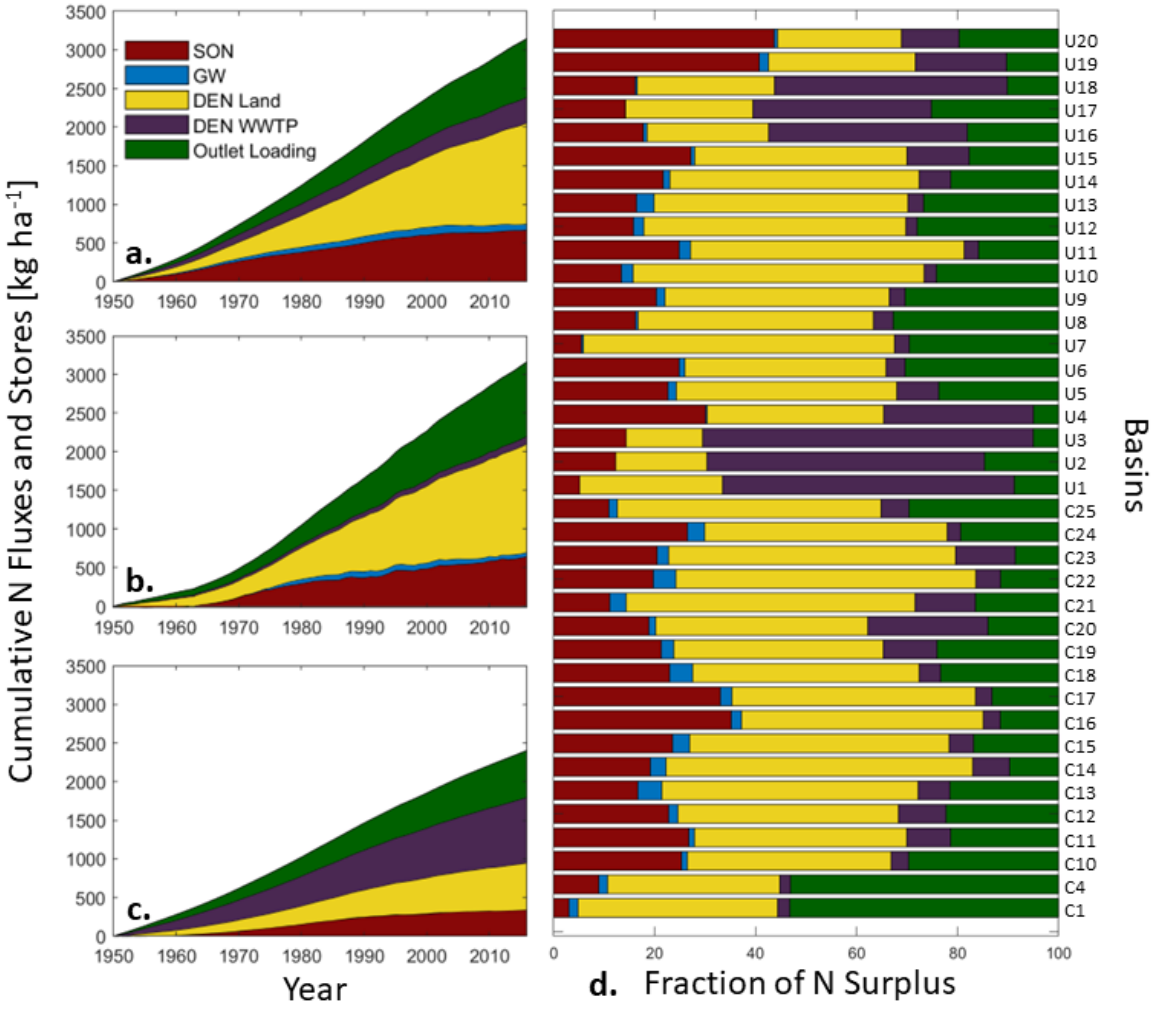

Figure 14: Fate of applied N since 1950: Cumulative N fluxes and N stores across the Lake Erie basin from 1950 to 2016 (N stores include groundwater and SON accumulation and N fluxes include cumulative stream N loading, WWTP N removal, and landscape denitrification) in the (a) Grand River, ON (C19), (b) Maumee River (U9), and (c) Cuyahoga River (U17). (d) The proportion of N attributed to each of the fluxes and stores is shown for modelled sub-watersheds ** Note, results are presented for only 38 of the 45 sub-watersheds. I omitted 7 sub-watersheds since SON accumulation patterns looked suspect in them, despite being able to describe outlet loadings (SON was negative in recent years, which is unrealistic and necessitates more investigation).

Next, I looked at how landscape features might affect the fate of N in a watershed over time. For each modelled sub-watershed I compared how percent tile drainage and percent agricultural area correlated to the fates of N. Tile drainage was significantly positively correlated ($R^2 = 0.56$,

$p<0.001$) with the proportion of N that is hydrologically released (rather than stored).As tile-drainage density increases, legacy N storage declines and is increasingly released directly into streams.. These results are consistent with the Grand River study, where high values of travel time (μ) correlated with high SON and GW accumulation, and where high levels of tile drainage correlated with low values of travel time (μ).

Chapter 4: Conclusions

4.1 Summary

The overall objective of this thesis was to understand legacy nitrogen dynamics across the transboundary LEB, using a combination of data synthesis and process modelling, I developed datasets and models for 45 sub-watersheds across the LEB, 25 in Canada and 20 in the U.S.

Across all 45 sub-watersheds, surplus N began to increase after 1950 and peaked between 1980 and 2000; ranging from 34 to 108 kg/ha. The source breakdown of this surplus varied across the LEB. In highly urban sub-watersheds, domestic waste N comprised the majority of N surplus, whereas, for the majority of the agricultural sub-watersheds, the rise in N surplus was driven by an increase in fertilizer application and high rates of biological N fixation. After the peak period, a steady decline in N surplus occurs across the majority of the sub-watersheds until 2010, which is likely driven by improved fertilizer use efficiency (more crop N uptake per applied fertilizer and manure). Flow-weighted N concentrations for the sub-watersheds do not respond linearly to changes in the N surplus; rather, they show a disconnected, lagged response.

To quantify the fluxes of N applied across the LEB, I developed and calibrated models for 45 sub-watersheds and simulated over a century of riverine N loading for each. Overall, the models performed well and were able to appropriately simulate N loading trajectories using only eight calibrated parameters. The median KGE and PBIAS for modelled vs measured loading across the sub-watersheds were 0.75 and 1.9% respectively. The models were also able to capture current-day SON. The median PBIAS for measured vs modelled SON was 12%.

I found that the calibrated model parameters vary considerably across the LEB. Groundwater travel times range from 5 to 35 years and was significantly negatively correlated with the amount of tile drainage in the sub-watershed. Soil and groundwater denitrification rates also vary across the LEB and are also negatively correlated with the degree to which tile drainage is used in the watershed. As more of a sub-watershed is drained artificially, water in the subsurface flows quicker, leaving less opportunity for N denitrification. Thus, more applied N ends up in the stream before it can undergo denitrification. Wastewater denitrification rates were positively correlated with the population density of sub-watersheds, so the more urban the watershed, the higher the wastewater denitrification rates. This is likely a result of larger, urban cities having larger, more sophisticated WWTPs that can remove a higher percentage of N through denitrification.

The stores of legacy N across the LEB have been increasing from 1950 to 2016. Sub-watersheds have experienced up to 952 kg/ha of legacy N storage (median: 603 kg/ha). Up to 910 kg/ha of N has been stored in the soil and as much as 187 kg/ha has been stored in the groundwater. Across all of the sub-watersheds, only 5% to 53% of applied N has reached the stream (20% median); the rest has been either denitrified or stored as legacy N. Among the sub-watersheds, up to 44% of surplus N has had the potential to build up as legacy N. The percentage of accumulated legacy N is correlated to the tile drainage of the watershed. Sub-watersheds with a higher density of tile drainage are correlated with shorter groundwater travel times and retain less N than those with less artificial drainage.

4.2 Implications and future work

4.2.1 Implications

The Lake Erie basin is a large, heterogeneous landscape that includes many land cover types and jurisdictions. By quantifying N surplus across the LEB and modelling N dynamics in multiple sub-watersheds, I were able to quantify N legacies across the watershed and what drives them. Watershed N management regulations that only set targets for N application (N surplus) do not account for N already stored as legacy across the watershed: large stores of soil organic N as well as N dissolved in slow-moving groundwater. Depending on a watershed's physical characteristics and land-management practices, N can remain in the system for decades before reaching the outlet (Van Meter et al., 2018; Ilampooranan et al., 2019; Liu, 2020). The thesis results have the potential to influence watershed management practices. By explicitly quantifying N legacies in Lake Erie sub-watersheds, stakeholders can consider legacy N stores when setting nutrient reduction targets to make reasonable and informed decisions about how to reduce N in the lake.

By modelling several sub-watersheds across the LEB, I were also able to capture the heterogeneity of N legacy patterns. This allows for a more local and targeted nutrient management approach for the watershed. One can identify the predominant storage type of legacy N in each sub-watershed to target management practices to. In agricultural sub-watersheds with ample legacy SON, cover crops and reduced fertilizer application rates could effectively reduce the amount of N loading in the stream. Sub-watersheds with slow travel times and, thus, higher groundwater N accumulation might benefit from the addition of wetlands to intercept the subsurface flow of N and provide the opportunity for denitrification. I have also

demonstrated how travel times in a sub-watershed influence how N is retained in the system; watersheds with quick travel times have shorter lag times and retain less N. Thus, watersheds with high SON stores and quick travel times (usually heavily tile drained watersheds) should be managed first, as reducing N in these sub-watersheds should, theoretically, lead to the fastest improvement in stream water quality.

Finally, the harmonized N surplus, soil, and landcover data for the LEB compiled here for the first time has the potential to facilitate further meaningful nutrient and water quality analyses. Models are often only applied to one side of the U.S./Canada border because of the lack of data-consistency between the countries. This thesis aggregated data from both sides of the border; this cross-border data can be clipped to sub-watersheds of varying scales across the LEB, and used for further analysis and modelling endeavours.

4.2.2 Future work

While this thesis was able to successfully model 45 sub-watersheds across the LEB and identified several trends between land cover characteristics and model parameters and results, more work is needed to further refine the results. First, calibration and parameter selection will need to be explored for sub-watershed models which had unexpected results (either with respect to model performance (section 3.2) or with respect to unusual SON legacy stores (section 3.4)). For these sub-watersheds, I need to explore parameter ranges or model assumptions to ensure I best capture their physical reality. Next, while this study covered many of the sub-watersheds in the LEB, some sub-watersheds remain unmodelled due to lack of N concentration or stream discharge data. For these areas, I can make use of the parameter relationships defined in section 3.3 and use parameter transfer techniques to estimate N legacy stores across the entire LEB.

Finally, once all the models have been refined, future sub-watershed simulations could consider scenarios with differing N surplus application changes (increases or decreases). Using these changes, the models could simulate how long it would take to achieve N loading reductions given different nutrient reduction strategies.

References

Agriculture and Agri-Food Canada, 2016a. Annual Crop Inventory

Agriculture and Agri-Food Canada, 2016b. Soil Landscapes of Canada.

Asadzadeh, Masoud, and Bryan Tolson. 2013. "Pareto Archived Dynamically Dimensioned Search with Hypervolume-Based Selection for Multi-Objective Optimization." *Engineering Optimization* 45 (12): 1489–1509.

Baily, A., L. Rock, C. J. Watson, and O. Fenton. 2011. "Spatial and Temporal Variations in Groundwater Nitrate at an Intensive Dairy Farm in South-East Ireland: Insights from Stable Isotope Data." *Agriculture, Ecosystems & Environment* 144 (1): 308–18.

Boden, T. A., G. Marland, and R. J. Andres. 2009. "GLOBAL, REGIONAL, AND NATIONAL FOSSIL-FUEL CO2 EMISSIONS." *Carbon Dioxide Information Analysis Center (CDIAC) Datasets*. https://doi.org/10.3334/cdiac/00001.

Boiko, O., Kagone S., Senay G.B., 2021, Soil properties dataset in the United States: U.S. Geological Survey data release, https://doi.org/10.5066/P9TI3IS8.

Byrnes, D. K., K. J. Van Meter, and N. B. Basu, 2020. "Typologies of Nitrogen Surplus Trajectories Using the New TREND-Nitrogen Dataset: Shifting Hotspots and Dominant Controls." In , 2020:H084–0018.

Byrnes, D. K., K. J. Van Meter, and N. B. Basu, 2022. "Trajectories Nutrient Dataset for Nitrogen (TREND-Nitrogen)." *https://figshare.com/articles/dataset/Trajectories_Nutrient_Dataset_for_Nitrogen_TREND-Nitrogen_/20915989*.

Chang, S.Y., D. K. Byrnes, K. J. Van Meter, and N. B. Basu. In Review. “Gridded Trend-Nitrogen Dataset: Long-term annual gridded nitrogen surplus across the United States (1930 - 2017)"

Chen, Dingjiang, Hong Shen, Mingpeng Hu, Jiahui Wang, Yufu Zhang, and Randy A. Dahlgren. 2018. “Chapter Five - Legacy Nutrient Dynamics at the Watershed Scale: Principles, Modeling, and Implications.” In *Advances in Agronomy*, edited by Donald L. Sparks, 149:237–313. Academic Press.

Cleveland, Cory C., Alan R. Townsend, David S. Schimel, Hank Fisher, Robert W. Howarth, Lars O. Hedin, Steven S. Perakis, et al. 1999. “Global Patterns of Terrestrial Biological Nitrogen (N2) Fixation in Natural Ecosystems.” *Global Biogeochemical Cycles* 13 (2): 623–45.

D’Elia, Christopher F., Morris Bidjerano, and Timothy B. Wheeler. 2019. “Population Growth, Nutrient Enrichment, and Science-Based Policy in the Chesapeake Bay Watershed.” In *Coasts and Estuaries*, 293–310. Elsevier.

Drury, C. F., J. Y. Yang, R. De Jong, X. M. Yang, E. C. Huffman, V. Kirkwood, and K. Reid. 2007. “Residual Soil Nitrogen Indicator for Agricultural Land in Canada.” *Canadian Journal of Soil Science*. https://doi.org/10.4141/s06-064.

Dubrovsky, Neil M., Karen R. Burow, Gregory M. Clark, Joann M. Gronberg, Pixie A. Hamilton, Kerie J. Hitt, David K. Mueller, et al. 2010. “The Quality of Our Nation’s Waters: Nutrients in the Nation's Streams and Groundwater, 1992-2004.” *Circular*. US Geological Survey. https://doi.org/10.3133/cir1350.

EPA. 2012. “2012 Edition of Drinking Water Standards and Health Advisories.”

www.epa.gov/sites/production/files/2015- 09/documents/dwstandards2012.pdf

Epa, U. S., and OW. 2014. “Mississippi river/Gulf of Mexico Hypoxia Task Force,” October. https://www.epa.gov/ms-htf.

Galloway, James N., and Ellis B. Cowling. 2021. “Reflections on 200 Years of Nitrogen, 20 Years Later.” *Ambio* 50 (4): 745–49.

Grimvall, Anders, Per Stålnacke, and Andrzej Tonderski. 2000. “Time Scales of Nutrient Losses from Land to Sea — a European Perspective.” *Ecological Engineering* 14 (4): 363–71.

Hamlin, Q. F., A. D. Kendall, S. L. Martin, H. D. Whitenack, J. A. Roush, B. A. Hannah, and D. W. Hyndman. 2020. “Quantifying Landscape Nutrient Inputs with Spatially Explicit Nutrient Source Estimate Maps.” *Journal of Geophysical Research. Biogeosciences* 125 (2). https://doi.org/10.1029/2019jg005134.

Helcom, Bsap. 2007. “HELCOM Baltic Sea Action Plan.” *Krakow, Poland* 15: 2007.

Hirsch, Robert M., Douglas L. Moyer, and Stacey A. Archfield. 2010. “Weighted Regressions on Time, Discharge, and Season (WRTDS), with an Application to Chesapeake Bay River Inputs.” *Journal of the American Water Resources Association* 46 (5): 857–80.

Ho, J.C., Stumpf, R.P., Bridgeman, T.B., Michalak, A.M., 2017. Using Landsat to extend the historical record of lacustrine phytoplankton blooms: A Lake Erie case study. Remote Sensing of Environment 191, 273–285. https://doi.org/10.1016/j.rse.2016.12.013

Hong, Bongghi, Dennis P. Swaney, and Robert W. Howarth. 2011. “A Toolbox for Calculating Net Anthropogenic Nitrogen Inputs (NANI).” *Environmental Modelling & Software* 26 (5): 623–33.

Hong, B., Swaney, D.P., 2013. NANI Accounting Toolbox ,Version 3.1.0.

Hong, B., Swaney, D.P., Howarth, R.W., 2013. Estimating Net Anthropogenic Nitrogen Inputs

to U.S. Watersheds: Comparison of Methodologies. Environmental Science & Technology 47, 5199–5207. https://doi.org/10.1021/es303437c

Hong, B., Swaney, D.P., Howarth, R.W., 2011. A toolbox for calculating net anthropogenic nitrogen inputs (NANI). Environmental Modelling & Software 26, 623–633. https://doi.org/10.1016/j.envsoft.2010.11.012

Hong, B., Swaney, D.P., McCrackin, M., Svanbäck, A., Humborg, C., Gustafsson, B., Yershova, A., Pakhomau, A., 2017. Advances in NANI and NAPI accounting for the Baltic drainage basin: spatial and temporal trends and relationships to watershed TN and TP fluxes. Biogeochemistry 133, 245–261. https://doi.org/10.1007/s10533-017-0330-0

Hong, B., Swaney, D.P., Mörth, C.-M., Smedberg, E., Eriksson Hägg, H., Humborg, C., Howarth, R.W., Bouraoui, F., 2012. Evaluating regional variation of net anthropogenic nitrogen and phosphorus inputs (NANI/NAPI), major drivers, nutrient retention pattern and management implications in the multinational areas of Baltic Sea basin. Ecological Modelling 227, 117–135. https://doi.org/10.1016/j.ecolmodel.2011.12.002

Iho, Antti, Marc Ribaudo, and Kari Hyytiäinen. 2015. “Water Protection in the Baltic Sea and the Chesapeake Bay: Institutions, Policies and Efficiency.” *Marine Pollution Bulletin* 93 (1-2): 81–93.

Ilampooranan, Idhayachandhiran, K. J. Van Meter, and Nandita B. Basu. 2019. “A Race against Time: Modeling Time Lags in Watershed Response.” *Water Resources Research* 55 (5): 3941–59.

Jaffe, Daniel A. 1992. “12 The Nitrogen Cycle.” In *International Geophysics*, edited by Samuel S. Butcher, Robert J. Charlson, Gordon H. Orians, and Gordon V. Wolfe, 50:263–84.

Academic Press.

Karimi, Rezvan, Sarah J. Pogue, Roland Kröbel, Karen A. Beauchemin, Timothy Schwinghamer, and H. Henry Janzen. 2020. “An Updated Nitrogen Budget for Canadian Agroecosystems.” *Agriculture, Ecosystems & Environment* 304 (December): 107046.

Kellogg, R.L., Lander, C.H., Moffitt, D.C., Gollehon, N., 2000. Manure Nutrients Relative to the Capacity of Cropland and Pastureland to Assimilate Nutrients: Spatial and Temporal Trends for the United States. U.S. Department of Agriculture

Knoben, W. J. M., Freer, J. E., and Woods, R. A., 2019. Technical note: Inherent benchmark or not? Comparing Nash–Sutcliffe and Kling–Gupta efficiency scores, Hydrol. Earth Syst. Sci., 23, 4323–4331, https://doi.org/10.5194/hess-23-4323-2019

Lee, M., S. Malyshev, E. Shevliakova, P. C. D. Milly, and P. R. Jaffé. 2014. “Capturing Interactions between Nitrogen and Hydrological Cycles under Historical Climate and Land Use: Susquehanna Watershed Analysis with the GFDL Land Model LM3-TAN.” *Biogeosciences* 11 (20): 5809–26.

Le Moal, Morgane, Chantal Gascuel-Odoux, Alain Ménesguen, Yves Souchon, Claire Étrillard, Alix Levain, Florentina Moatar, et al. 2019. “Eutrophication: A New Wine in an Old Bottle?” *The Science of the Total Environment* 651 (Pt 1): 1–11.

Liu, S., Wei, Y., Post, W. M., Cook, R. B., Schaefer, K., and Thornton, M. M. 2013. The Unified North American Soil Map and its implication on the soil organic carbon stock in North America, Biogeosciences, 10, 2915–2930, https://doi.org/10.5194/bg-10-2915-2013.

Liu, J., K. J. Van Meter, M. M. McLeod, and N. B. Basu. 2021. “Checkered Landscapes:

Hydrologic and Biogeochemical Nitrogen Legacies along the River Continuum." *Environmental Research Letters: ERL [Web Site]* 16 (11): 115006.

McCourt, Sibeal, and Graham K. MacDonald. 2021. "Provincial Nitrogen Footprints Highlight Variability in Drivers of Reactive Nitrogen Emissions in Canada." *Environmental Research Letters: ERL [Web Site]* 16 (9): 095007.

Meals, Donald W., Steven A. Dressing, and Thomas E. Davenport. 2010. "Lag Time in Water Quality Response to Best Management Practices: A Review." *Journal of Environmental Quality* 39 (1): 85–96.

Michigan Department of Environmental Quality, 2020. MIDEQ Data

National Hydrological Service, 2016. Canadian hydrometric Data

Ohio Environmental Protection Agency, 2020.

Ontario Ministry of Environment, Conservation, and Parks. 2020. "Provincial Water Quality Monitoring Network (PWQMN)." DataStream. https://datastream.org/dataset/f3877597-9114-4ace-ad6f-e8a68435c0ba.

"OSTRICH Optimization Software Toolkit." n.d. Accessed November 5, 2021. http://www.civil.uwaterloo.ca/envmodelling/Ostrich.html.

Ramankutty, Navin, and Jonathan A. Foley. 1999. "Estimating Historical Changes in Global Land Cover: Croplands from 1700 to 1992." *Global Biogeochemical Cycles*. https://doi.org/10.1029/1999gb900046.

Reutter, J.M. 2019. Lake Erie: Past, Present, and Future. In Encyclopedia of Water, P. Maurice (Ed.). https://doi.org/10.1002/9781119300762.wsts0085

Roser, Max, Hannah Ritchie, and Esteban Ortiz-Ospina. 2013. "World Population Growth." *Our*

World in Data, May. https://ourworldindata.org/world-population-growth

Sarrazin, Fanny J., Rohini Kumar, Nandita B. Basu, Andreas Musolff, Michael Weber, Kimberly J. Van Meter, and Sabine Attinger. 2022. "Characterizing Catchment-scale Nitrogen Legacies and Constraining Their Uncertainties." *Water Resources Research* 58 (4). https://doi.org/10.1029/2021wr031587.

Smil, V., 1999. Nitrogen in crop production: An account of global flows. Global Biogeochemical Cycles 13, 647–662. https://doi.org/10.1029/1999GB900015

Statistics Canada, 2016a. Canadian Census of Agriculture.

Statistics Canada, 2016b. Table 32-10-0039-01 Fertilizer shipments to Canadian agriculture markets, by nutrient content and fertilizer year, cumulative data.

Statistics Canada, 2016c. Canadian Census of Population.

Statistics Canada, 2016d. Table 32-10-0359-01 Estimated areas, yield, production, average farm price and total farm value of principal field crops, in metric and imperial units

Swaney, Dennis P., Robert W. Howarth, and Bongghi Hong. 2018. "Nitrogen Use Efficiency and Crop Production: Patterns of Regional Variation in the United States, 1987–2012." *The Science of the Total Environment* 635 (September): 498–511.

Tolson, Bryan A., and Christine A. Shoemaker. 2007. "Dynamically Dimensioned Search Algorithm for Computationally Efficient Watershed Model Calibration." *Water Resources Research* 43 (1). https://doi.org/10.1029/2005wr004723.

Us Epa, O. W. 2014. "Mississippi river/Gulf of Mexico Hypoxia Task Force," October. https://www.epa.gov/ms-htf.

U.S. Geological Survey, 2020, National Water Information System data available on the World

Wide Web (USGS Water Data for the Nation) https://waterdata.usgs.gov/nwis/

Van Meter, Kimberly J., and Nandita B. Basu. 2015. “Catchment Legacies and Time Lags: A Parsimonious Watershed Model to Predict the Effects of Legacy Storage on Nitrogen Export.” *PloS One* 10 (5): e0125971.

Van Meter, K. J., N. B. Basu, and P. Van Cappellen. 2017. “Two Centuries of Nitrogen Dynamics: Legacy Sources and Sinks in the Mississippi and Susquehanna River Basins: Two Centuries of Nitrogen Dynamics.” *Global Biogeochemical Cycles* 31 (1): 2–23.

Van Meter, K. J., N. B. Basu, J. J. Veenstra, and C. L. Burras. 2016. “The Nitrogen Legacy: Emerging Evidence of Nitrogen Accumulation in Anthropogenic Landscapes.” *Environmental Research Letters: ERL [Web Site]* 11 (3): 035014.

Vero, Sara E., Nandita B. Basu, Kimberly Van Meter, Karl G. Richards, Per-Erik Mellander, Mark G. Healy, and Owen Fenton. 2018. “The Environmental Status and Implications of the Nitrate Time Lag in Europe and North America.” *Hydrogeology Journal* 26 (1): 7–22.

Wang, Rong, Daniel Goll, Yves Balkanski, Didier Hauglustaine, Olivier Boucher, Philippe Ciais, Ivan Janssens, et al. 2017. “Global Forest Carbon Uptake due to Nitrogen and Phosphorus Deposition from 1850 to 2100.” *Global Change Biology* 23 (11): 4854–72.

Wurtsbaugh, Wayne A., Hans W. Paerl, and Walter K. Dodds. 2019. “Nutrients, Eutrophication and Harmful Algal Blooms along the Freshwater to Marine Continuum.” *WIREs Water*. https://doi.org/10.1002/wat2.1373.

Appendix A: Data Summary for non-hydrological N input and N output data

Country	Input/Output Category	Data Required	Spatial Resolution, Extent	Temporal Resolution, Time Span	Data Source
Canada	**Biological N Fixation**	Biological N fixation rates	-	-	Byrnes et. al, 2020; Byrnes et. al, 2022
	Livestock Manure N	Livestock headcounts	County, Canada	Census Years, 1901-2016	Canadian Census of Agriculture
		Livestock nutrient parameters	-	-	Byrnes et. al, 2020; Byrnes et. al, 2022
	Atmospheric N Deposition	Atmospheric N deposition	1.2 x 1.2 degrees, Global	Annual, 1850,1960, 1970, 1980, 1990, 1997-2013	Wang et. al, 2017
		Carbon emissions	Country resolution, Global	Annual, 1785-2014	Carbon Dioxide Information Analysis Center (CDIAC)
	Mineral N Fertilizer	Fertilizer Salces	Provincial scale, Canada	Annual, 1951-2016	Stats Canada, Table: 32-10-0039-01
	Domestic N Waste	Population	County scale, Canada	Census Years, 1901-2016	Canadian Census of Agriculture
			Provincial scale, Canad	Census Years, 1951-2016	Canadian Census
	Crop N Uptake	Crop area	County scale, Canada	Census Years, 1901-2016	Canadian Census of Agriculture
		Crop yield	Provincial scale, Canada	Annual, 1908-2016	Stats Canada, Table: 32-10-0359-01
		Crop nutrient parameters	-	-	Byrnes et. al, 2020; Byrnes et. al, 2022; Hong and Swaney, 2013
	Downscaling Landcover Data	Gridded Land Cover Data	30 x 30 m, Canada	Annual, 2011-2016	Annual Crop Inventory Canada (ACI)
U.S.A	**Biological N Fixation**	Biological N fixation	County Scale, U.S.	Annual 1930-2017	Byrnes et. al, 2022
	Livestock Manure N	Livestock N excretion	County Scale, U.S.	Annual 1930-2017	Byrnes et. al, 2022
	Atmospheric N Deposition	Atmospheric N deposition	1.2 x 1.2 degrees, Global	Annual, 1850,1960, 1970, 1980, 1990, 1997-2013	Wang et. al, 2017
		Carbon emissions	Country resolution, Global	Annual, 1785-2014	Carbon Dioxide Information Analysis Center (CDIAC)
	Mineral N Fertilizer	Mineral N Fertilizer	County Scale, U.S.	Annual 1930-2017	Byrnes et. al, 2022
	Domestic N Waste	Domestic N waste	County Scale, U.S.	Annual 1930-2017	Byrnes et. al, 2022
	Crop N Uptake	Crop N uptake	County Scale, U.S.	Annual 1930-2017	Byrnes et. al, 2022
	Downscaling Landcover Data	Gridded Land Cover Data	250 x 250 m, U.S.	Annual, 1938-1992; 2001, 2003, 2006, 2008, 2011, 2013, 2016	Sohl et al, 2016; NLCD, USGS

Appendix B: Summary of all median performance metrics for each sub-watershed

Basin	KGE	PBIAS Load	PBIAS SON	**Basin**	KGE	PBIAS Load	PBIAS SON	**Basin**	KGE	PBIAS Load	PBIAS SON
C1	0.67	0.03	0.06	**C17**	0.71	0.04	0.07	**U8**	0.55	0.04	0.13
C2	0.78	0.01	0.14	**C18**	0.86	0.04	0.19	**U9**	0.6	0.04	0.1
C3	0.68	0.03	0.07	**C19**	0.9	0.03	0.16	**U10**	0.82	0.03	0.12
C4	0.76	0.18	0.26	**C20**	0.65	0.04	0.15	**U11**	0.9	0.04	0.1
C5	0.69	0.02	0.53	**C21**	0.91	0.02	1.28	**U12**	0.73	0.06	0.09
C6	0.71	0.03	0.09	**C22**	0.89	0.01	0.48	**U13**	0.88	0.03	0.06
C7	0.87	0.02	0.1	**C23**	0.9	0.03	0.19	**U14**	0.18	0.15	0.13
C8	0.68	0.03	0.05	**C24**	0.78	0.05	0.04	**U15**	0.42	0.09	0.03
C9	0.52	0.1	0.03	**C25**	0.84	0.03	0.04	**U16**	0.65	0.03	0.03
C10	0.86	0.04	0.12	**U1**	0.32	0.04	1.89	**U17**	0.31	0.03	0.16
C11	0.7	0.04	0.13	**U2**	0.5	0.02	0.13	**U18**	0.69	0.04	0.12
C12	0.77	0.05	0.13	**U3**	0.44	0.34	3.78	**U19**	0.89	0.04	0.03
C13	0.82	0.03	0.22	**U4**	0.72	0.18	1	**U20**	0.86	0.03	0.23
C14	0.76	0.03	0.23	**U5**	0.9	0.02	0.01				
C15	0.89	0.03	0.24	**U6**	0.75	0.04	0.09				
C16	0.76	0.04	0.02	**U7**	0.48	0.42	0.02				

Appendix C: Summary of all sub-watersheds and their cumulative N fluxes and stores, including sub-watersheds omitted in the main analysis (starred).